EUROPEAN COMMISSION

Community research

PAMINA
Performance Assessment Methodologies in Application to Guide the Development of the Safety Case

(Contract Number: FP6-036404)

PA approach to gas migration
DELIVERABLE (D-N°:3.2.1)

Magdalena Dymitrowska (IRSN)
Alain Genty (CEA)
Dmitriy Lukin (NRI)
Martin Navarro (GRS)
Eef Weetjens (SCK·CEN)
Editors: J. Grupa, T.J. Schröder (NRG)

Date of issue of this report: **26/11/2009**

Start date of project: **01/10/2006** Duration: 36 Months

Project co-funded by the European Commission under the Euratom Research and Training Programme on Nuclear Energy within the Sixth Framework Programme (2002-2006)		
Dissemination Level		
PU	Public	X
RE	Restricted to a group specified by the partners of the [PAMINA] project	
CO	Confidential, only for partners of the [PAMINA] project	

Foreword

The work presented in this report was developed within the Integrated Project PAMINA: **P**erformance **A**ssessment **M**ethodologies **IN** **A**pplication to Guide the Development of the Safety Case. This project is part of the Sixth Framework Programme of the European Commission. It brings together 25 organisations from ten European countries and one EC Joint Research Centre in order to improve and harmonise methodologies and tools for demonstrating the safety of deep geological disposal of long-lived radioactive waste for different waste types, repository designs and geological environments. The results will be of interest to national waste management organisations, regulators and lay stakeholders.

The work is organised in four Research and Technology Development Components (RTDCs) and one additional component dealing with knowledge management and dissemination of knowledge:

- In RTDC 1 the aim is to evaluate the state of the art of methodologies and approaches needed for assessing the safety of deep geological disposal, on the basis of comprehensive review of international practice. This work includes the identification of any deficiencies in methods and tools.

- In RTDC 2 the aim is to establish a framework and methodology for the treatment of uncertainty during PA and safety case development. Guidance on, and examples of, good practice will be provided on the communication and treatment of different types of uncertainty, spatial variability, the development of probabilistic safety assessment tools, and techniques for sensitivity and uncertainty analysis.

- In RTDC 3 the aim is to develop methodologies and tools for integrated PA for various geological disposal concepts. This work includes the development of PA scenarios, of the PA approach to gas migration processes, of the PA approach to radionuclide source term modelling, and of safety and performance indicators.

- In RTDC 4 the aim is to conduct several benchmark exercises on specific processes, in which quantitative comparisons are made between approaches that rely on simplifying assumptions and models, and those that rely on complex models that take into account a more complete process conceptualization in space and time.

The work presented in this report was performed in the scope of RTDC 3.

All PAMINA reports can be downloaded from http://www.ip-pamina.eu.

Table of Contents

1. Introduction 4
2. Methodologies to assess the impact of gas generation and migration on the safety of the repository 6
   2.1 Potential safety issues 7
   2.2 Modelling of gas generation and migration in PA 9
      2.2.1 Gas generation 9
      2.2.2 Distribution of gaseous compounds over the water and gas phase 10
      2.2.3 Two-phase flow in a rigid porous media 11
      2.2.4 Gas flow due to pathway dilation 14
      2.2.5 Overpressurization and macro-fractures 14
3. Work performed within WP3.2 16
   3.1 Supercontainer concept 18
      3.1.1 SCK·CEN 20
      3.1.2 CEA 25
      3.1.3 IRSN 27
   3.2 Couplex-Gaz case 30
      3.2.1 CEA 31
      3.2.2 IRSN 33
   3.3 Czech granite concept 35
   3.4 German hypothetical clay concept 39
4. Discussion 50
   4.1 Potential safety issues 51
   4.2 Modelling of gas migration processes 53
5. Conclusions 56
   Appendix A Summary of the contribution of CEA 58
   Appendix B Summary of the contribution of GRS 60
   Appendix C Summary of the contribution of IRSN 63
   Appendix D Summary of the contribution of NRI 67
   Appendix E Summary of the contribution of SCK·CEN 68
   References 71

1. Introduction

In a nuclear waste repository, the generation of gas by the waste, by corrosion of steel containers and overpacks or other processes is a long standing issue. The gas produced may affect the performance of a repository system in several ways: local high gas pressures may induce faster transport of radionuclides, pressure build-up may change the physico-chemical behaviour of enclosing materials such as buffer and backfill and accumulation of gas in a volume near to the waste may impact the heat removal of heat generating waste. To assess the effects of gas generation, understanding of the balance between gas generation and gas migration is essential.

The generation of gas has been dealt with in previous EC-programmes, e.g. the NF-Pro project [1]. The aim of the Work Package 3.2 of RTDC-3 of the PAMINA integrated project is therefore to improve the understanding of the migration of gaseous compounds on process level and to improve the representation of such processes in performance assessment (PA) models.

This report addresses the work done in WP3.2 of PAMINA: '*PA approach to gas migration*'. Six partners have contributed to this work package: CEA, GRS, IRSN, NRI, SCK·CEN and NRG.

This report has the following aims:

- to introduce the reader to the issue of gas generation and migration in PA
- to show how gas generation and migration is addressed in PA
- to give an overview of the work done in WP3.2 of PAMINA
- to reflect on the work done by the partners, to find parallels, and to identify different approaches
- to serve as a point of reference to the partner specific reports
- to point out open questions

Within this work package, each of the partners performed an analysis of the gas migration behaviour in nuclear waste repository systems. The primary objective of the contributions differs between the partners, covering code development and testing, representation of conceptual models in computational codes, generic test calculations and design specific analyses. Although this work package is not intended to perform benchmark calculations, some contributions addresses similar repository designs and offers therefore an opportunity to make some (limited) quantitative comparisons of different model implementations.

As the milestone reports of the individual partners already contain detailed in-depth information on the systems they analysed, the methods they used, and the assumptions they made, this report aims to give a general overview of the way gas migration is addressed in the context of PA. Using this perspective, in the next chapter a general introduction on the current state-of-the-art of the relevant processes behind gas migration and the way they are addressed in PA is given. Chapter 3 presents the work performed by the individual partners in the present work package. In Chapter 4, the results of the individual partners are compared, and their relevance for PA is discussed. Chapter 5 gives a synthesis of the results attained in this work package and gives a general conclusion on the modelling of gas migration. Summaries of the individual contributions of the partners can be found in the Appendix.

2. Methodologies to assess the impact of gas generation and migration on the safety of the repository

The generation of gas and migration of these gaseous compounds is, similar to e.g. thermo-mechanical analyses, the assessment of the solubility of the waste matrix and the modelling of reactive transport of radionuclides in pore water, a safety relevant issue that will feed into the *Safety Case* [2].

Any Safety Case has to be developed in a number of iterations, and the first iteration step is generally done by a generic desk top study that addresses the overall feasibility of a disposal concept and gives a first demonstration of the general safety of the concept on the long term. Subsequent iterations can be a result of introducing more site and design specific details, but can also be a result of changes in the scope of the Safety Case, such as new regulations, new features of the facility, or new ideas on how a Safety Case should be presented. In each iteration, safety relevant aspects are studied independently by several process level models each focusing on a number of specific aspects only. All processes have to be combined in the Safety Case, which often requires a simplified representation of the process models.

The iterative character of the Safety Case is also necessary because a more detailed modelling of the processes for a given repository design may lead to the identification of new safety relevant issues: in the present case, generic process knowledge on gas generation and migration is available, but only by a careful modelling of both processes in one model, the resulting gas pressure build-up can be estimated properly. For example, the gas pressure build-up may cause mechanical damage to repository components, and may increase the migration of radionuclides, thus represents a potentially relevant safety issue. Once the relevance of gas pressure build-up in a given repository design is demonstrated, the necessity may appear to improve process knowledge and develop tools to quantify the issues more precisely.

The iterative nature of calculations performed for the Safety Case thus strongly influences the focus of the work performed on a particular subject and the way it is analyzed. Since various disposal system designs addressed are in different iteration steps, the scopes of the studies addressed in this report may differ: some studies focus on analyzing the safety related consequences of gas migration for a given design, while other studies are improving some features of the calculations tools to resolve more accurately specific issues found in previous iterations steps.

In the next Section, the potential safety issues related to the generation and migration of gas are discussed. Section 2.2 gives a limited overview on the relevant processes behind gas migration and discussed briefly the way they are implemented in process level code used for performance assessment.

2.1 Potential safety issues

In this chapter we describe the safety issues that may arise within the most common description of the gas migration processes. A nuclear waste disposal facility will contain a range of different compounds that potentially may lead to the generation of gas. In general, anaerobic corrosion of metals is the dominant gas generating process. Iron containing metals are used as package material for high level waste and other waste fractions and can be present as activated or contaminated metals in the intermediate and low level waste packages. After closure of the facility all oxygen will be reduced by chemical reactions within a few years, and anaerobic corrosion of metals will start when the metals come into contact with water. The anaerobic corrosion of iron results in the production of hydrogen gas. The corrosion rate depends on environmental conditions, the availability and composition of water, the composition and surface structure of the metal and the size of the contact area between metal and water. Other processes that may lead to gas generation are (biological) conversion or radiolysis of organic compounds, radiolysis of water, and decay of radioactive materials to gaseous daughter nuclides.

The generation of gas leads to an increase of the gas pressure if the generation rate is higher than the migration rate of gas out of the disposal areas. The main processes that affect the migration of gas away from the source are (1) diffusion of gas dissolved in pore water and (2) advective gas transport through (partly saturated) pores. Gas migration by diffusion is assumed not to affect the functioning of the engineered barrier system (EBS) or the host rock. The effects of advective gas transport on the functioning of the EBS or the host rock are generally small, too.

However, when the gas generation rate exceeds the transport capacity of the enclosing materials over longer periods, the gas pressure will rise. In certain clay formations that are considered as a host rock for a disposal facility, a process called '*pathway dilation*' may occur [3, 4]. This process influences the pore size distribution within the clay, but does not result in macro-fracturing.

If the gas pressure exceeds the minimal principal stress condition of a material, fracturing of the engineered barriers or host rock may occur. This event is termed *overpressurization* [5] and may lead to the formation of new pathways (macro-fractures) along which radionuclides might be transported.

The following potential safety issues attributed to the generation and migration of gaseous compounds have been identified [6]:

Gas Driven Nuclide Migration

Gas flow may lead to pore water movements. If radionuclides are dissolved in the pore water, the gas flow may facilitate increased nuclide migration.

Migration of radioactive Gases

Some wastes contain (or produce) gaseous radionuclides. If gas formation leads to an advective gas flow, radionuclides in the gas phase may migrate (together with the other gases) faster than radionuclides dissolved the water phase.

Overpressurization

In some cases the generated gas may not be able to migrate into the surrounding material if this has a high gas entry pressure, such as low permeable clays and bentonite. If there is a continuous net gas generation (i.e. there is more gas generated than removed by e.g. dissolution and diffusion) and the gas volume can not expand, the pressure of the gas may increase to a level beyond the hydrostatic pressure and may approach value in the order of magnitude of the local lithostatic pressure. Such pressure levels may lead to structural damages and may result in the development of preferential flowpath, most likely along the interfaces between EBS and along the excavation damage zone (EDZ).

Retarded resaturation

After closure of a repository in granite or clay, the EDZ is getting resaturated and parts of the backfill and EDZ can get saturated. In the case of an early onset of the gas generation, the saturation of the EBS and EDZ may be inhibited and therefore the EBS may not achieve the expected thermomechanical properties (e.g. by swelling of bentonite plugs). Inhomogeneities may also lead to changes in the stress conditions, especially in case of swelling clays. As a consequence, this may lead to mechanical instability or damage of the EBS.

Thermal properties of the system

The water content of porous materials influences the heat conductivity of these materials. Gas generation may lead to desaturation of pore volumes in the engineered barrier system or the enclosing host rock, which may have an impact on the temperature distribution around the heat emitting high level waste (HLW). An analysis of the gas migration behaviour is necessary to ensure that the enhanced temperatures will not exceed the maximum design temperatures of any repository component.

Flammability hazard

The formation of flammable gases, like H_2 produced by anaerobic corrosion of metal or methane produced by the conversion of organic material in intermediate level waste or low level waste (ILW or LLW), is a potential safety issue during the operational phase or the early post-closure phase.

2.2 Modelling of gas generation and migration in PA

The basic knowledge for analysing gas generation and migration was already available in the EVEGAS (1996), MEGAS (1997), and PEGASUS (1995) projects [7, 8, 9, 10]. Calculation methodologies have been developed to estimate the generation of gas, the amount of 'free gas' around the gas sources (the waste and the containers), the gas removal rates, and the resulting gas pressure. The models can also be used to evaluate far field effects, such as (hypothetical) breakthrough of radioactive gases to the surface. Thus, a number of methods are available to evaluate the potential safety issues as described in the previous section.

In the last decade, progress has been made regarding the ability to model two phases flow inside a radioactive waste disposal facility more efficiently and detailed by the ability to analyse finer meshes in either 2D or 3D, leading to more a more accurate representation of a disposal by using unstructured meshes instead of rectangular meshes and by explicitly addressing the heterogeneity and anisotropy of the repository structures. The drawback of those progresses was the emergence of new numerical problems linked to large and highly heterogeneous and anisotropic systems [11].

Concerning the experimental support to prove the validity of the classical, Darcy-based two-phase flow model for modelling gas migration in saturated clay, no significant progress has been made recently. Moreover, there is also a lack of experimental support for the constitutive two-phase flow relations at low gas saturation level - which is the relevant saturation range for gas phase flow in the host rock. Attention has been drawn to the mechanism of pathway dilation in the last years which also has been stressed in the Swiss 'Projekt Entsorgungsnachweis' [12]. Several conceptual models have been developed, but still experimental support is needed to gain a sufficient physical support for these models. Thus the testing of modelling outcome against experiments is a relevant issue, and some work will be done in the recently started EU-FP7 FORGE project [13], in which the various models for gas generation and migration will be compared with experimental results and in which detailed process level knowledge will be developed.

In the next sections, the processes behind gas generation and migration are summarized and the way these are implemented in present PA models is discussed.

2.2.1 Gas generation

Gas generation rates that are applied in PA are commonly based on experimental observations on laboratory scale that are extrapolated to *in situ* conditions. The underlying models are based on chemical reaction equations, with the rate constants derived from experimental observations. As shown in other studies [1, 14], gas generation rates are characterised by large uncertainties because of the complexities of the long term (bio-) chemical evolution of the system. Still, several uncertainties are present in the prediction of gas formation rates and extrapolation to a repository system: uncertainties can be introduced by the fact that even very small gas formation rates may be relevant for the system performance on the long scale (thousands of years), uncertainties may be present in the prediction of amounts of water that may be available for anaerobic corrosion or biological processes, uncertainties are present in the determination of size of the contact surface between water and corroding material, and uncertainties may exist on the long term evolution of the local chemistry (e.g. pH) at these interfaces. To cover these uncertainties and to avoid the use of complex geochemical codes in PA related studies, several approaches are possible. E.g., gas generation can be modelled by using next to a central estimate for the formation rate constants also a lower and an upper bound value.

In PAMINA, the generation of gas has not been studied extensively, because this item has been dealt with in detail in the NF-Pro project [1].

2.2.2 Distribution of gaseous compounds over the water and gas phase

By the dissolution of gaseous compound in the water phase, the water phase can act as a sink for large fractions of the gases that can be produced in a repository. The amount of gas that is taken up by the water phase is dependent on a number of factors, like the solubility of a compound or the composition of the water phase.

The distribution of a gaseous compound over the water and gas phase is generally described by Henry's law:

$$p_i = K_i \cdot x_i \qquad \text{Eq. 1}$$

with p_i the partial pressure of the compound, K_i the Henry constant and x_i the mole fraction of a compound in water. For an inert gas like N_2 the use of Henry's law is in most cases sufficient to estimate the distribution over the water and gas phase, because this system behaves similar to the thermodynamical (ideal) system that is the basis for Henry's law. In case of a reactive gas, e.g. CO_2, much more gas than calculated by Henry's law can be dissolved in water, because once CO_2 is dissolved in the water phase, it is getting hydrated. This results in a decrease of the mole fraction of free CO_2-species in the water phase, leading to the uptake of more gaseous CO_2 to re-establish the phase distribution described by Eq. 1. This process continues until the free CO_2-species in the water phase is in equilibrium with all other CO_2 containing compounds. The reaction behaviour of a species in groundwater can thus be quite complex and can be estimated by speciation and adsorption theory, but for gases like H_2, the use of Henry's law may be considered sufficient because it gives a conservative estimate of the pressure reduction by the dissolution of H_2 into the water phase.

2.2.3 *Two-phase flow in a rigid porous media*

In most backfill materials (e.g. cementitious materials, unsaturated or partly saturated bentonite) and some host rock materials (e.g. granite), *two-phase flow* can occur. The two-phase flow condition is characterised by a state in which the pore volume is partly filled with gas, and partly filled with water, in a way that a flow network for both gas and water exists. According to the two-phase flow theory, the permeability of the porous material for both fluids depends on the intrinsic permeability of the porous medium, the viscosity of the fluid, and also on the degree of saturation.

Gas migration can be modelled by conventional two-phase flow models, where the porous medium is static and the gas flow is determined by the geometry and layout of the open pore space (porosity and tortuosity), the capillary pressure functions (e.g. van Genuchten model [15]) and the relative permeability functions (e.g. Corey's model for deriving relative permeability's from the liquid or gas saturation of the pores [16]). Usually, dissolution and diffusion of gases in the water phase is included in the equations.

A general way to calculate the migration of a component in a porous medium is the use of a mass balance equation. The mass balance can be expressed as:

$$\frac{\partial M^{\kappa}}{\partial t} = -\mathrm{div}(F^{\kappa}_{advection} + F^{\kappa}_{diffusion}) + q^{\kappa} \qquad \text{Eq. 2}$$

with M^{κ} the local mass density of component κ, $F^{\kappa}_{advection}$ and $F^{\kappa}_{diffusion}$ the advective and diffusive flow density of component κ and q^{κ} the source term of component κ.

For the repository systems under consideration in PAMINA WP3.2, the relevant components are water and hydrogen gas, where the latter is present in the gas phase and/or dissolved in water phase. The presence of water in the gas phase is not considered in most of the simulations and has no relevant influence on the outcome of the calculations.

Unlike diffusion of gas, gas flow in a repository component by advection will only happen when the gas saturation in an adjacent component is large enough to displace pore water, or equivalently, when the gas pressure exceeds the gas entry pressure of a saturated porous component. The conditions under which this will happens are explained in greater detail in subsequent sections.

Purely diffusive transport

At relatively small gas pressures no advective flow is induced by the generation of gas due to the gas entry thresholds. Still, gaseous compounds that are dissolved in the water phase can migrate away from the source by diffusion in the water phase. Diffusion is a concentration dependent process and is described by Fick's law:

$$F^{\kappa}_{diffusion} = -D_{\kappa} \frac{\partial C_{\kappa}}{\partial x}$$ Eq. 3

with C_κ the concentration of a component in water, D_κ the diffusion rate constant and x the distance. Generally, diffusion processes have a very limited capacity with respect to the transport of materials compared to advective transport.

Two-phase advective flow in porous media

At higher gas pressures, advective transport may take place. Advective transport is a far more effective transport mechanism than diffusion. For practical purposes, diffusive transport can often be ignored if advective transport takes place. Eq. 2 can then be simplified by removing the diffusion term $F^{\kappa}_{diffusion}$.

For a rigid porous medium, porosity ϕ [-] can be defined as the fraction of the open pore spaces V_v [m^3] of an elementary representative porous media volume V_r [m^3] by Eq. 4:

$$\phi = \frac{V_v}{V_r}$$ Eq. 4

The phase saturation S_α [-] can be defined as the fraction of phase α volume V_α [m^3] to the void volume:

$$S_\alpha = \frac{V_\alpha}{V_v}$$ Eq. 5

The velocity U_α [m·s^{-1}] can be defined by the Darcy equation:

$$\overline{U}_\alpha = -\overline{K}\left(\frac{K_{r\alpha}}{\mu_\alpha}\left(\mathrm{grad}(p_\alpha) - \rho_\alpha g\, \mathrm{grad}(z)\right)\right)$$ Eq. 6

where $\overline{K}$ [m^2] is the absolute permeability tensor; $K_{r\alpha}$ [-] is the relative permeability function; μ_α [kg·m^{-1}·s^{-1}] is the viscosity; and p_α [Pa] is the (partial) pressure of the phase α. Density driven transport is taken into account by multiplying the density ρ_α with the gravity constant g [9.81 m·s^{-2}] and the vertical distance z [m] in upward direction.

Insertion of Eq. 6 into Eq. 2 for each phase α results into:

$$\phi \frac{\partial}{\partial t}(S_\alpha \rho_\alpha) = -\mathrm{div}\left(\rho_\alpha \overline{U}_\alpha\right) + q_\alpha$$ Eq. 7

with ρ_α [kg·m^{-3}] the density of phase α, and q_α [kg·m^{-3}·s^{-1}] a source term.

When the Darcy equation is used to describe two-phase flow, the permeability is not a constant value but depends on the interaction between both phases and the porous media. In a conventional rigid porous system the capillary pressures arises from the pressure difference across curved interfaces that are formed between the gas and water phases within the pore spaces. The local capillary pressure cause the gas phase to access the larger sized pores before the smaller sized pores, so that, as the gas saturation increases and smaller sized pores spaces become gas filled, the capillary pressure increases. The capillary pressure p_c is defined as:

$$p_c = p_g - p_l \qquad \text{Eq. 8}$$

with p_g the gas pressure and p_l the pressure of the liquid phase.

Capillary pressure is usually modelled by the empirical *van Genuchten* expression [15], where the phase saturation S_α is only dependent on the residual liquid and gas saturation. The effective phase saturation Se_α of the phase α is defined as:

$$Se_\alpha = \frac{S_\alpha - S_{\alpha r}}{1 - S_{lr} - S_{gr}} \qquad \text{Eq. 9}$$

where S_{lr} and S_{gr} are the residual liquid and gas saturation respectively.

The capillary pressure is calculated in the van Genuchten approach by

$$p_c^{vG} = p_r^{vG}\left(Se_l^{-1/m} - 1\right)^{1-m} \qquad \text{Eq. 10}$$

where p_c^{vG} is the (positive) capillary pressure according to the van Genuchten model, p_r^{vG} the apparent gas entry pressure, m the shape parameter (m≈0.33) and Se_l the effective phase saturation Se_α for phase $\alpha = l$.

A clear distinction has to be made between the "*gas entry pressure*" parameter p_r^{vG} of the van Genuchten expression (Eq. 10) and the pressure threshold for the inflow of a gas phase or capillary pressure p_c in Eq. 8: in a two-phase flow model, a threshold pressure for gas flow can be introduced by means of the capillary pressure and the relative gas permeability. The gas phase can enter the saturated clay only if the gas pressure is higher than the gas entry pressure. This implies that the relative gas permeability is larger than zero above the entry pressure (capillary pressure $p_c>0$) and zero below it (capillary pressure $p_c \leq 0$). In case of the van Genuchten approach, there is no rigorous threshold for the mobility of the gas phase (see Eq. 10: $p_c^{vG} \approx 0$ if $S_{e,g} \approx 0$). Possible ways to implement gas entry thresholds in a two-phase flow model are discussed in detail in [17].

Simulations of GRS performed within WP3.2 show that the choice of the capillary pressure function and the relative gas permeability does not only affect the gas entry pressure but also the pressure-dependent capacity of the rock to store a gas phase, which has a strong influence on the gas migration process. For this reason, GRS used for their simulation a modified van Genuchten function (see Section 3.4).

2.2.4 Gas flow due to pathway dilation

In a repository for radioactive wastes which is located in an indurated clay stone, gas pressures will rise if gas production rates exceed the outflow of gas from the repository by diffusion or visco-capillary flow. Well before gas pressures reaches the minimal principal stress condition and macroscopic fractures form, gas may intrude into the rock by creating additional (secondary) pore space, without causing any macro-fracturing, by dilating existing pores. This mechanism is called *pathway dilation* [3] and may comprise growth and opening of microscopic pores or the connection of existing pores into the flow passages. Pathway dilation is usually thought to take place above certain pressure thresholds but due to the small-scale heterogeneity of stresses and material properties in mudrocks or bentonite, there is probably no sharp transition to the dilated state.

With respect to the materials present in deep geological repositories, the process of pathway dilation has been investigated experimentally most intensively on bentonite [18, 19], but there is also experimental evidence for pathway dilation in indurated [20] and plastic clays [21]. Indications for the existence of the process of pathway dilation are volumetric strains during gas entry and non-Darcy linear relation between gas flow and gas pressure gradient registered in experiments.

Although this process may be relatively straightforward from a phenomenological point of view, there is yet no general agreed modelling approach for this effect. This owes not only to the fact that the processes leading to pathway dilation can be very complex on microscopic process-scale and difficult to distinguish experimentally. A general approach to model pathway dilation might not be possible due to the large variety of physico-chemical properties of argillaceous materials which can modify the involved processes from case to case. Furthermore, the integration of this effect into a transport model is not straightforward. Within the present work package, GRS developed a conceptual model for pathway dilation and integrated this model into a two-phase flow code. Both the conceptual model and the code integration can be found together with the results of their calculations in Section 3.4.

2.2.5 Overpressurization and macro-fractures

If all gas transport processes introduced above have not sufficient capacity to remove the gas at the same rate as the gas is generated, gas pressures will increase and may exceed the minimal principal stress conditions, resulting in *overpressurization* [3, 4] and macro-fractures. In case of clay, pathway dilation is expected to occur before the gas pressure exceeds the minimal principal stress conditions and may have sufficient transport capacity to keep the gas pressure low enough to prevent overpressurization. But if gas flows through a cementitious (concrete) part of the EBS, overpressurization may occur. The gas may then escape through a preferential flow path, which will most likely be situated along the EDZ.

Within this work package, no contributor has incorporated overpressurization and the formation macro-fractures into their models. However, although this process is not dealt with quantitatively, from the gas pressures calculated in the different contributions, it can be estimated if overpressurization is likely to occur.

3. Work performed within WP3.2

In order to investigate the relevance of the phenomena described in the previous sections for repository safety, the partners within PAMINA's WP3.2 have defined several calculation cases that are considered to be representative for the in-situ conditions of the individual repository designs. For argillaceous host rocks, SCK·CEN [22, 23, 24], CEA [25] and IRSN [26] analysed the Belgian *Supercontainer* concept, CEA [27] and IRSN [26] analysed the *Couplex-Gaz* benchmark [28] and GRS [17, 29] analysed a hypothetical repository design. NRI [30, 31] contributed an analysis of the Czech repository design in granite.

Figure 1 gives a schematic overview of the general system components that are common to all calculation cases performed in the framework of PAMINA. Generally, the waste is enclosed in a steel container. In most of the concepts, the waste container is surrounded by a steel overpack or liner. Both, container and overpack/liner are the major source of gas generation. Between the waste and the host rock, one or several engineered barrier components are considered, consisting either of bentonite and/or concrete. In some cases, also a (second) steel liner or overpack is considered to be present in this area, resulting in an additional source of hydrogen gas.

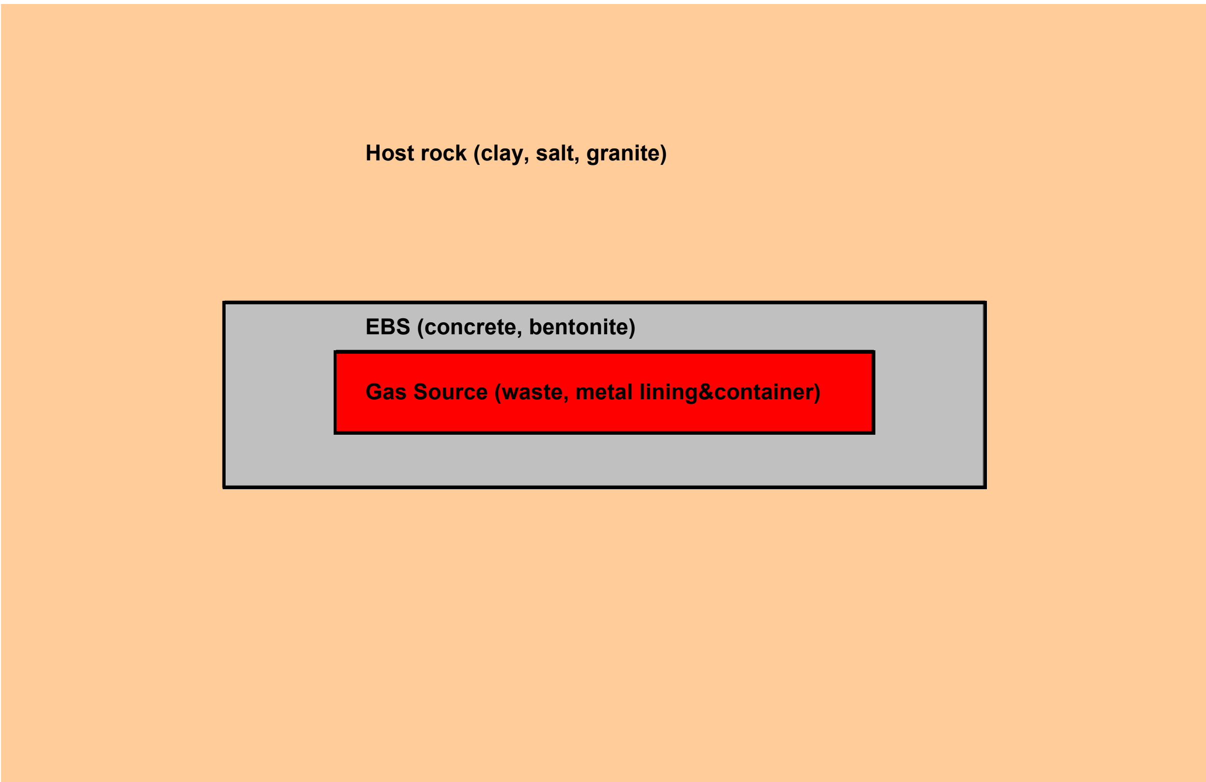

Figure 1: Schematic overview of a generic repository model

In the following sections, the calculations and analyses performed by the five partners are summarized. Table 1 summarizes the main features of the repository systems considered by the partners for the different calculation cases. A summary of the partner's contribution can also be found in the Appendix. For a more elaborated description, we refer to the partners individual Milestone reports indicated in Table 1.

Table 1: Overview of the calculation cases

	SCK·CEN	CEA	IRSN	CEA	IRSN	GRS	NRI
system analysed	Belgian *Supercontainer* repository concept			*Couplex-Gaz* benchmark with gallery		generic far-field analysis	borehole
host rock	Boom Clay			Callovo-Oxfordian clay		clay	granite
waste category	HLW			ILW		HLW	HLW
waste matrix	vitrified waste			*n.d.*		*n.d.*	spent fuel
container/ overpack	carbon steel			carbon steel		steel	carbon steel with 6 mm Ni alloy layer
EBS	carbon steel/OPC-concrete/cementitious backfill/concrete lining			concrete/bentonite plug		*n.d.*	bentonite bricks/ concrete plug
gas source	corrosion of container/overpack			corrosion of container/ overpack and metallic waste parts		corrosion of container/ overpack	corrosion of container/ overpack
gas solubility/ gas diffusion in water phase	yes	no	no	no	no	yes	yes
two-phase Darcy flow	yes			yes		yes	yes
pathway dilation	no			no		yes	no
considered gas	H_2			H_2		H_2	H_2
computational code(s) used	*COMSOL PORFLOW TOUGH2 Code Bright*	*Cast3m*	*MiGasTra*	*Cast3m*	*MiGasTra*	*TOUGH2* (modified)	*GoldSim TOUGH2*
PAMINA milestone reports	M3.2.7 M3.2.15 M3.2.16 [22, 23, 24]	M.3.2.3 [25]	M3.2.9 [26]	M3.2.10 [27]	M3.2.9 [26]	M3.2.13 M3.2.14 [17, 29]	M3.2.6 M3.2.8 [30, 31]

n.d: not defined

3.1 Supercontainer concept

A system based on the Belgian Supercontainer concept [32, 33] was analysed by SCK·CEN [22, 23, 24], CEA [25] and IRSN [26]. In this concept two COGEMA-containers, packed in a steel overpack, are enclosed in a concrete buffer with a diameter of 1.9 m (Figure 2).

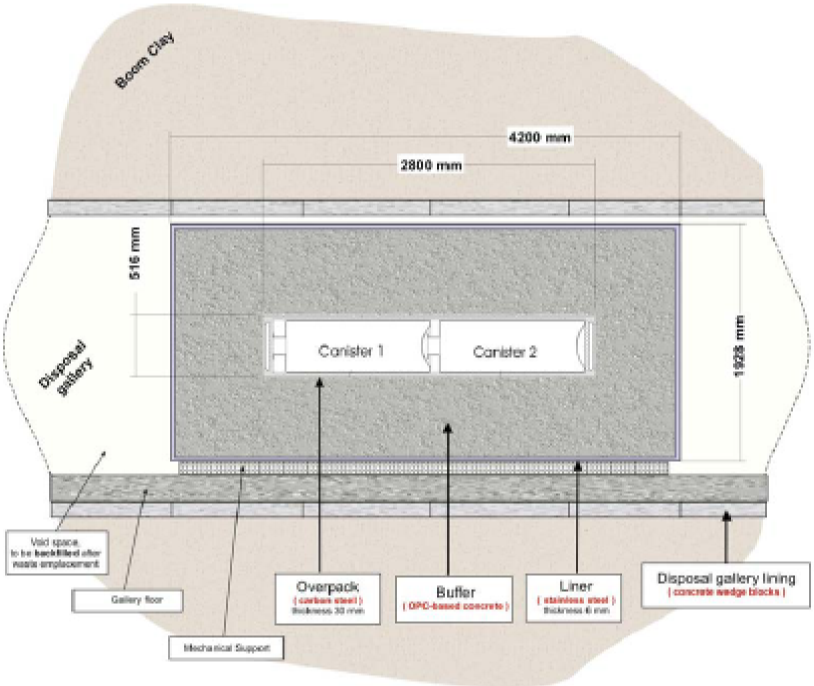

Figure 2: Longitudinal section of the Supercontainer design [24]

A simplified axi-symetrical 2D model representation of this concept is given in Figure 3. Table 2 summarized the dimensions of the different system compartments and in Table 3 the material properties are given. In the next sections, the contribution of each of the three partners is summarized.

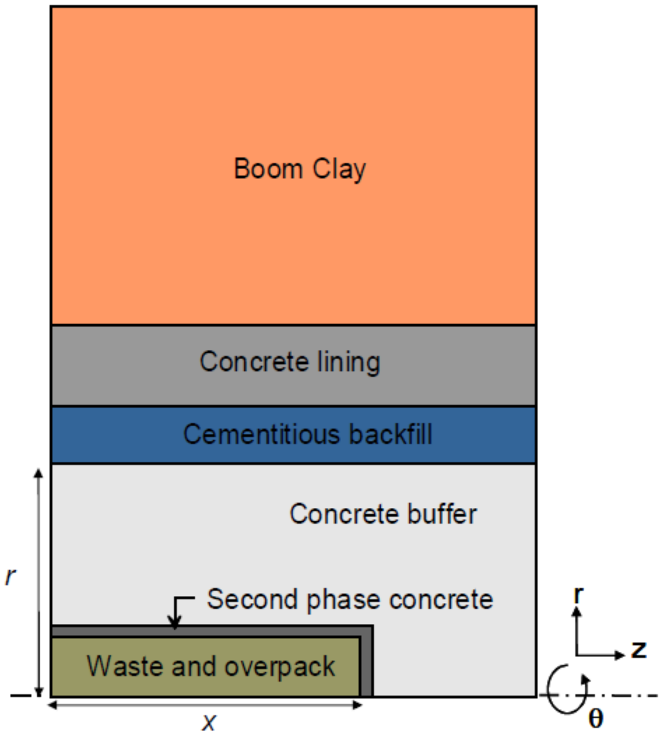

Figure 3: Model representation of the Supercontainer concept [25]

Table 2: Dimensions of the Supercontainer concept

material	maximal radial extend [m]	maximal axial extend [m]
waste & overpack	0.258	1.34
2nd phase concrete	0.308	1.39
concrete buffer	1.014	2.1
cementitious backfill	1.265	2.1
concrete lining	1.615	2.1
Boom Clay	4.0*/40**	2.1

* CEA/IRSN - size of the calculation grid

** SCK·CEN

Table 3: Material parameters for the Supercontainer model

parameter	2nd phase concrete	concrete buffer	cementitious backfill	concrete lining	Boom Clay
porosity ϕ [-]	0.300	0.104	0.300	0.104	0.391
permeability k [m^2]	$4.6 \cdot 10^{-17}$	$4.0 \cdot 10^{-21}$	$4.6 \cdot 10^{-17}$	$4.6 \cdot 10^{-17}$	$4.6 \cdot 10^{-19}$
van Genuchten parameter:					
shape parameter m [-]	0.43	0.43	0.43	0.43	0.355
residual liquid saturation S_{lr} [-]	0.25	0.25	0.25	0.25	0.20
residual gas saturation S_{gr} [-]	0.2	0.2	0.2	0.2	0.174
air entry pressure p_a [MPa]	0.5	0.5	0.5	0.5	2.83

3.1.1 SCK·CEN

The objective of SCK·CEN in the present work package is to explore gas issues in the context of a Safety Case by means of a case study, based on new Belgian Supercontainer concept for the disposal of vitrified high-level waste (HLW) in Boom Clay. At SCK·CEN, a series of 1D and 2D radial transport simulations have been carried out with the numerical codes *PORFLOW* [34] and *COMSOL* [35] to calculate the largest possible diffusive hydrogen fluxes from the near field into the Boom Clay [22, 23, 24]. A detailed two-phase flow analysis with the code *TOUGH2* [37, 38] was performed to assess the evolution of pressure, saturation and temperature in the repository and its environment [22, 23, 24].

Anaerobic corrosion of steel EBS components is found to be the most significant source of gas production within the near field of a repository for vitrified HLW [36]. Figure 4 show the three different H_2 gas generation scenario's analysed by SCK·CEN, based on two different corrosion rates (0.1 μm/a and 0.01 μm/a) and one temperature-dependent scenario.

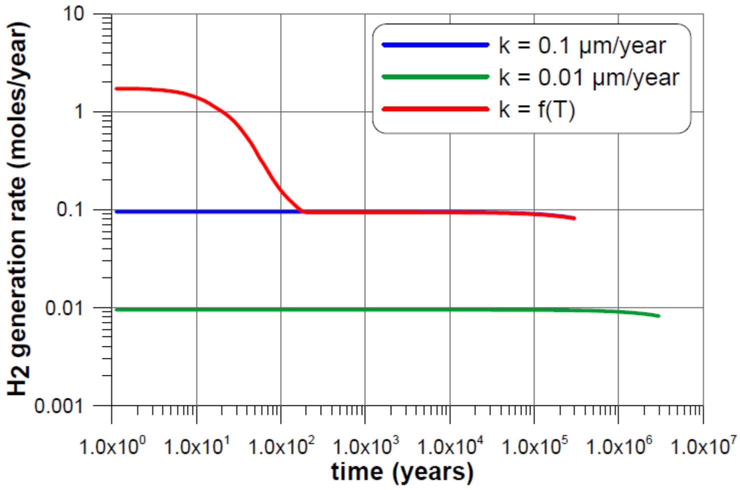

Figure 4: Gas generation scenario's for the diffusive removal analysis by SCK•CEN [24]

In the first part of the analysis, SCK·CEN estimates the largest possible diffusive hydrogen flux. The hydrogen concentration (near the overpack radius) was estimated by:

- assuming that the gas solubility linearly depends on the corresponding partial pressure of the gas, following Henry's law
- assuming that the partial pressure of hydrogen is equal to the in situ hydrostatic pressure (23 bars).

It should be noted that this is an oversimplified and conservative calculation at constant pressure, mainly while in reality gradually more and more hydrogen could dissolve in the pore water if the pressure increases.

The amount of hydrogen that can dissolve in the pore water at that pressure is 0.018 mol/L. For dissolved H_2, two apparent diffusion coefficients D of $5{\cdot}10^{-10}$ $m^2{\cdot}s^{-1}$ and $5{\cdot}10^{-11}$ $m^2{\cdot}s^{-1}$ were tested.

Figure 5 and Figure 6 show the calculated cumulative fluxes compared to the cumulative H_2 production rates for D=$5{\cdot}10^{-10}$ $m^2{\cdot}s^{-1}$ and D=$5{\cdot}10^{-11}$ $m^2{\cdot}s^{-1}$, respectively. Figure 5 shows that only in case of a temperature dependent gas production, the cumulative diffusive migration is not sufficient, for a relatively short period of time, to remove all the gas from the EBS (at the overpack and in the Supercontainer buffer) at the rate the gas is produced. Likewise, it can be seen from Figure 6 that, in the short term, only the EBS will be subject to increased gas pressures in case of a temperature dependent gas production. However, due to the assumed low diffusion coefficient, also in the longer term, increased gas pressures will now dominate the EBS, because the concentration gradient in the Boom Clay has flattened and the quasi-steady-state diffusive migration is not sufficient to remove the produced gas from the EBS (up to the interface with Boom Clay).

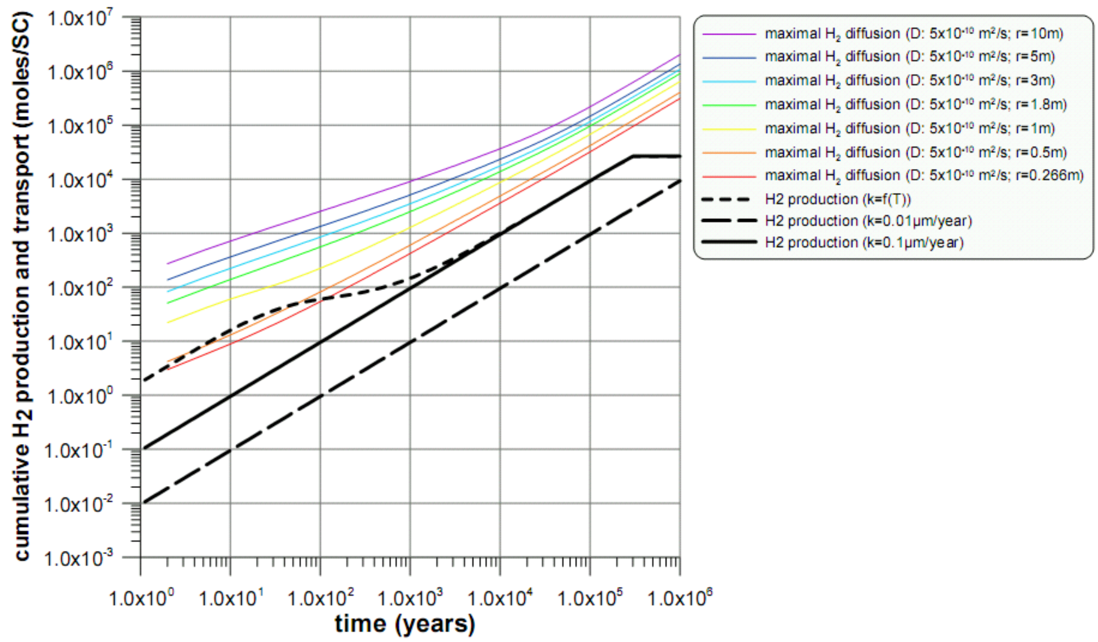

Figure 5: Maximal cumulative diffusive migration (D=5·10^{-10} m^2·s^{-1}) of dissolved H_2 versus cumulative H_2 production (in mol/Supercontainer) [24]

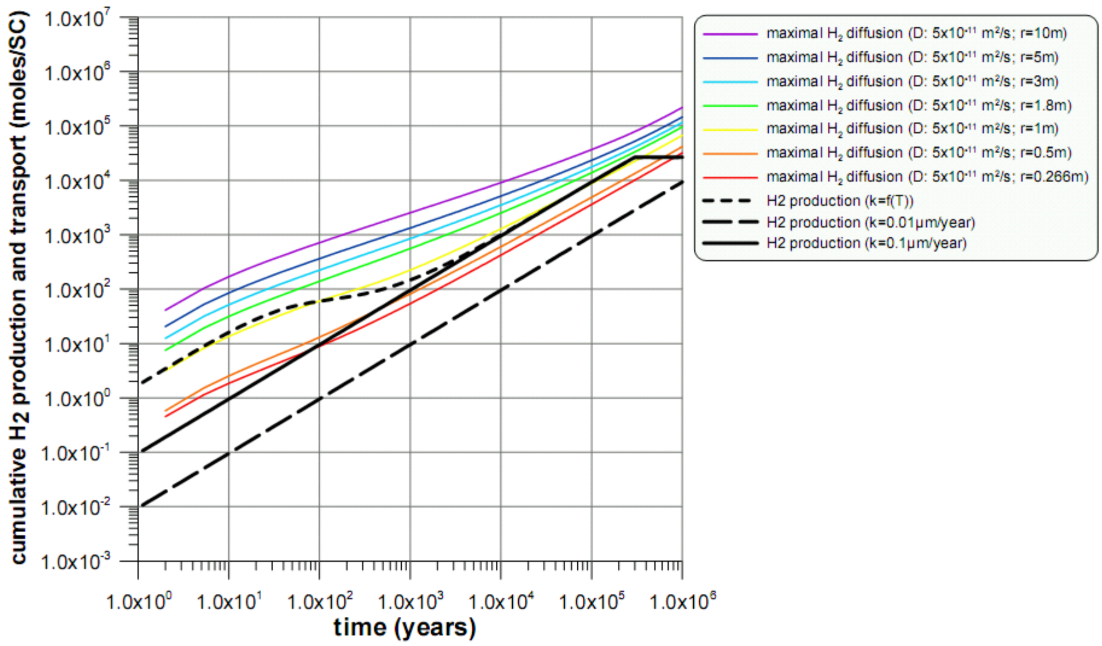

Figure 6: Maximal cumulative diffusive migration (D=5·10^{-11} m^2·s^{-1}) of dissolved H_2 versus cumulative H_2 production (in mol/Supercontainer) [24]

In general, these figures show that the cumulative hydrogen production does not exceed the capacity of the enclosing Boom Clay (which is found at r > 1.6 m) to remove the dissolved gas by diffusion in pore water for both diffusion coefficient values.

However, due to the lower cumulative flux in the long term, the required surface area for diffusion increases up to the radius of r=1.8 m, which is at the EBS/Boom Clay interface. Furthermore, it is possible that a free gas phase is generated soon after repository closure within the EBS. It should be noted that this is an oversimplified and conservative calculation at constant pressure, while in reality gradually more and more hydrogen could dissolve in the pore water if the pressure increases. Therefore, a more advanced and less conservative approach is used in the second step of the analysis, described below.

To evaluate the possible gas pressures attained in the near field and the corresponding degree of desaturation, a complementary two-phase-flow analysis was performed. However, the emphasis was on gaining insight in the behaviour of the system, and in particular testing the robustness of the system by using a variety of source term formulations and bounding values of the buffer permeability.

The gas calculations are performed with the *TOUGH2* code [37, 38]. The computational domain is discretized by 40 elements in the z-direction and 79 elements in the r-direction (Figure 3). The model is bounded by four boundaries. SCK·CEN assumed that 40 m vertical distance will provide sufficient length so that the primary variables could be fixed to constant value at the outer radial (r=40 m) boundary. Pressure and temperature are therefore fixed to 2.2 MPa and 15.7°C, respectively. All other boundaries are defined as *no flow* boundaries due to symmetry properties of the model shown in Figure 3. The simplified initial pressure conditions are divided into two parts. In the Boom clay a constant initial pressure of 2.2 MPa is assumed, whereas all engineered barriers (lining, backfill, buffer, waste and overpack) are at normal atmospheric pressure (0.1 MPa). For practical reasons, H_2 generation is assigned to the second phase concrete. Three gas terms are considered: a constant source, a step source and a temperature dependent source (Figure 7).

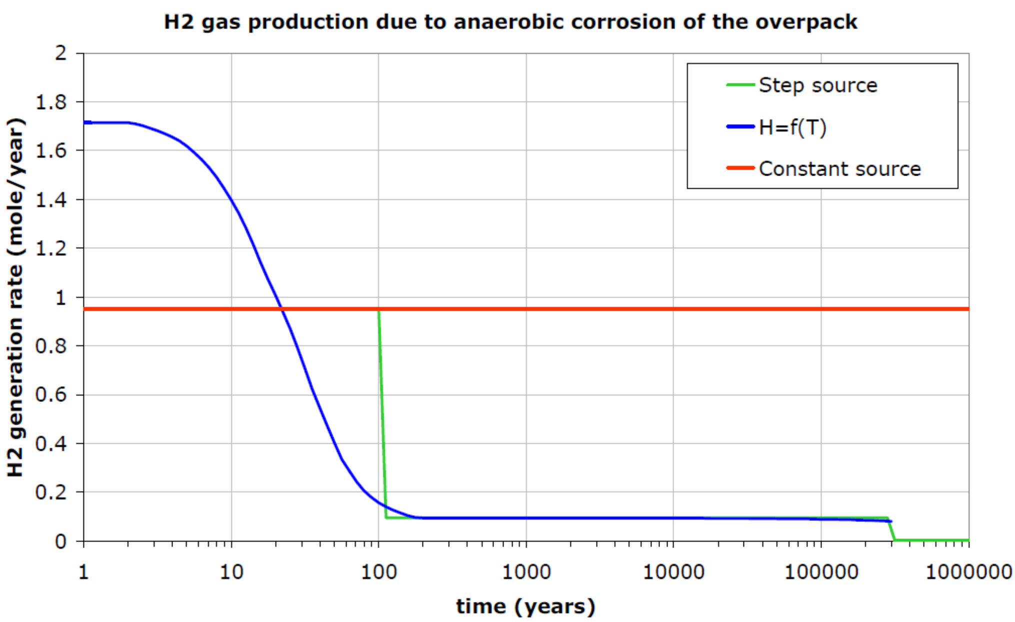

Figure 7: Gas generation scenario's for the multiphase analysis by SCK·CEN [24]

The model accounted for the temperature dependency of the H_2 solubility, the H_2 diffusion and the H_2 viscosity. By varying the gas source term, the heat source term and the permeability of the buffer, six different calculation cases were analysed (Table 4).

Table 4: Calculation cases considered by SCK·CEN

gas source	heat source	buffer permeability
constant	-	$4.6 \cdot 10^{-19}$ m^2
	-	$4.6 \cdot 10^{-21}$ m^2
step function	-	$4.6 \cdot 10^{-19}$ m^2
	f(t)	
f(t)	-	$4.6 \cdot 10^{-19}$ m^2
	f(t)	$4.6 \cdot 10^{-19}$ m^2
		$4.6 \cdot 10^{-21}$ m^2

The influence of temperature on the gas production process can be substantial but the overall influence of temperature on the gas transport process is small (Figure 8). The implementation of a heat source results in a slightly increased total pressure, mainly due to thermal expansion of both water and gas phase. The degree of gas saturation is not significantly higher compared to the isothermal case. In case of a high-permeability buffer, thermal expansion of the pore water causes slightly higher water pressures, whereas the pressure increase was considerably higher in the low-permeability case. However, this could be a consequence of the sequential modelling of the resaturation process and the gas generation and transport in a heated saturated environment: in reality, with a low-permeability buffer, the resaturation process will take longer (20 to 80 years depending on initial saturation degree), and the temperatures will already be much lower. Besides, the behaviour of the solid phase (concrete, clay) in this model is greatly simplified through the use of a storage coefficient approach.

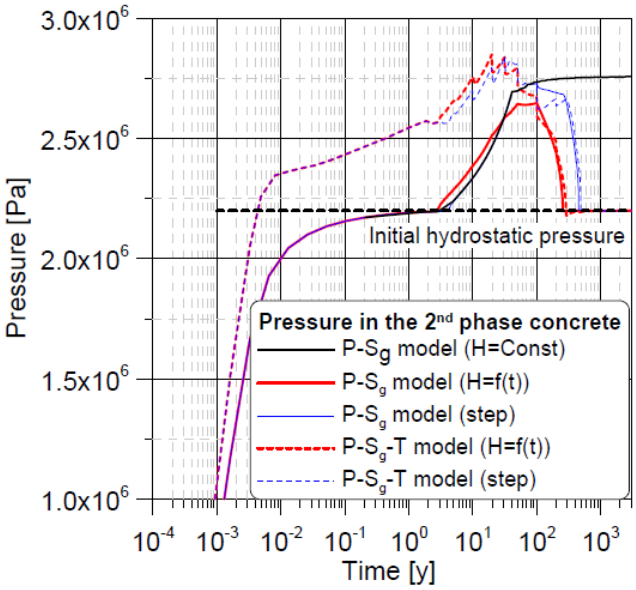

Figure 8: Comparison of pressure evolutions for different source terms calculated by SCK·CEN [24]

In all considered cases, the presence of a gas phase remains very local, *i.e.* within the EBS, and the Boom clay is not subject to a significant pressure increase (which was already indicated by the simplified diffusive mass-balance calculations). In the most realistic case, the maximum gas pressure reaches 2.85 MPa in the concrete filler after 20 years of gas production. The corresponding gas saturation is 20%. To have an idea of the physical impact of such a gas pressure, this value should be compared with the tensile strength of the concrete buffer. If the found value exceeds the concrete strength (which is not expected), cracks could form.

3.1.2 CEA

The main objective of CEA's analysis of the Supercontainer concept is to test the ability of two-phase flow codes to calculate gas pressures and saturation evolution with time by using *Cast3m* including a two-phase flow code developed by CEA [39]. Two cases were analyzed, with the first one based on the Belgian Supercontainer concept [25].

A two-phase flow calculation was performed, with the liquid phase and the solid matrix assumed to be incompressible, and the other phase follows the ideal gas law. The relative permeabilities and capillary pressure are described by the van Genuchten model. For the model geometry and material properties see Figure 3, Table 2, and Table 3. Modelling calculations are performed under isothermal conditions at T=289 K. In the cementitious backfill, concrete lining, and Boom Clay, CEA assumed fully saturated conditions, and inside the container unsaturated conditions at atmospheric pressure were used. Unlike SCK·CEN, CEA did not account for the dissolution and diffusion of H_2 in the water phase (Table 1). For the generation of gas, values of 0.093 mol/a and 0.095 mol/a are used for the waste container and the steel liner (Figure 2), respectively.

CEA analysed the long time behaviour of the gas pressure. Calculation results indicate that the total saturation of the system takes about 320'000 years (Figure 9). The saturation front propagates from the initial saturated area toward the inner part of the system. Gas pressure evolution in the system is found to be faster than water pressure and reached equilibrium in less than 5000 years [25].

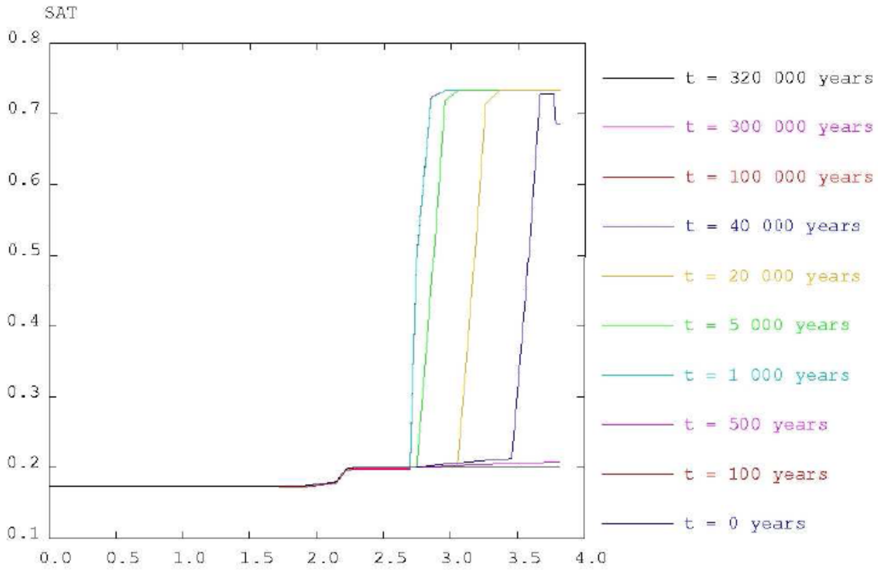

Figure 9: Gas saturation as function of the radial distance [m] from external clay boundary (waste is on the right at x=4 m) for several calculation times as calculated by CEA [25]

The gas pressure inside second phase concrete and concrete buffer has a maximum value at 40'000 years before it decreases again (Figure 10). No clear impact of the gas source term linked to the steel liner was found. Some additional computations conducted by CEA without this "liner" source term resulted in comparable results, except that the gas pressure build-up is faster, taking into account the "liner" source term.

Some small saturation oscillations as well as small pressure oscillations are obtained in CEA's computations. Those small numerical artefacts may results from the choice of time step evolution (geometric progression) that lead to regular time step cuttings in order to reach a fast fixed point algorithm convergence (less than 20 iterations), but may also stems from the use of non-regular hexahedrons mesh cells.

The maximum pressure calculated by CEA is about 2.5 MPa, a value in accordance with the values found by SCK·CEN (Figure 8). The maximum pressure was found by CEA in the second phase concrete (left part of Figure 10; x=4), which is in accordance with the results of SCK·CEN, too.

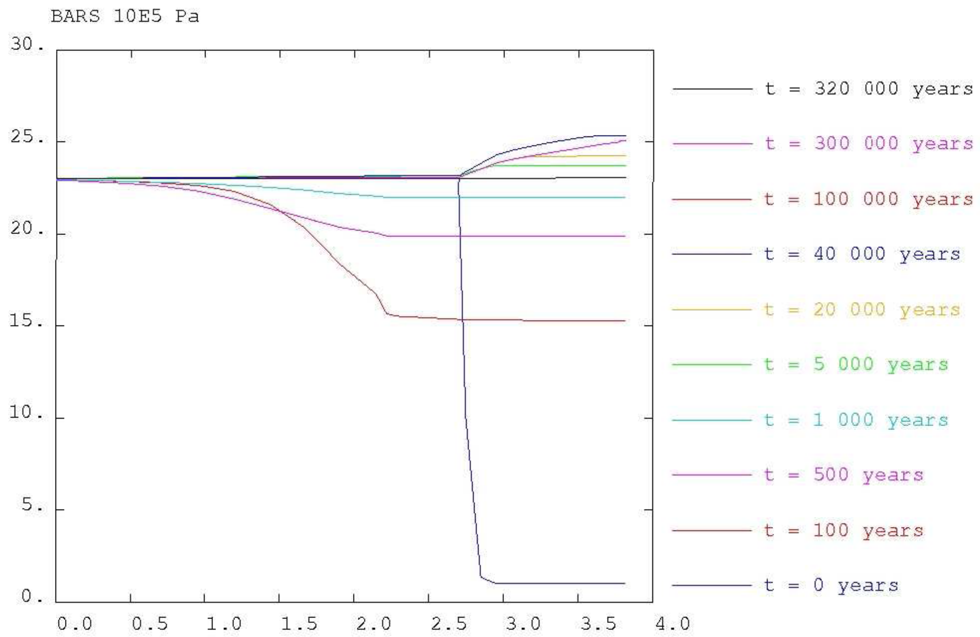

Figure 10: Gas pressure as function of the radial distance [m] from external clay boundary (waste is on the right at x=4 m) for several calculation times as calculated by CEA [25]

3.1.3 IRSN

The main goal of IRSN is the validation of the two-phase flow code *MiGasTra* [40], using the Belgian Supercontainer concept as a base for their first calculation case [27]. The calculation was prepared together with CEA (Section 3.1.2) in order to compare the outcomes of the codes.

For the calculations, the liquid phase and the solid matrix are assumed incompressible, and the gas phase follows the ideal gas law. The mathematical model includes mass conservation laws for both one-component phases supplemented by generalized Darcy equations for each phase. The relative permeabilities and capillary pressure are described by the van Genuchten model. For the model geometry and material properties see Figure 3, Table 2, and Table 3. Modelling calculations are performed under isothermal conditions at T=289 K. In the concrete lining and in the Boom Clay, IRSN assumed fully saturated conditions, and inside the container unsaturated conditions at atmospheric pressure were used. For the generation of gas, values of 0.093 mol/a and 0.095 mol/a are used for the waste overpack and the steel liner, respectively. A two-phase flow calculation without dissolution and evaporation effects was performed. Some modifications were introduced with respect to the original test case (and to the CEA calculation case): the axial symmetry was replaced by a plane 2D geometry and the simulations were conducted with all residual saturations equal to zero. In order to keep a similar dynamical behaviour of the system, the gas source term had to be modified. The surface density of gas production in the axi-symmetrical case was calculated and then applied to the 2D case. Since all residual saturations were set to zero, the initial conditions were taken to be equal to initial values of reduced water saturation, as used by the other partners (in order to have the same initial capillary pressure values).

The simulations were conducted up to 1'000'000 years, however only very slight variation of the system state was observed after 20'000 years, and the system did not resaturate at the final time.

Figure 11 and Figure 12 give the variations in gas pressure and water saturation in different materials. It can be noted that the Boom Clay desaturates very quickly (in less than 100 years) due to the establishment of the capillary pressure equilibrium with the concrete liner. At a later stage, the inside of the Supercontainer starts to resaturate. Within 100 years of system evolution the gas pressure has become equal to hydrostatic pressure everywhere in the system. The gas pressure reaches its maximum of 2.35 MPa at 40'000 years and slowly decreases to the final hydrostatic pressure of 2.3 MPa.

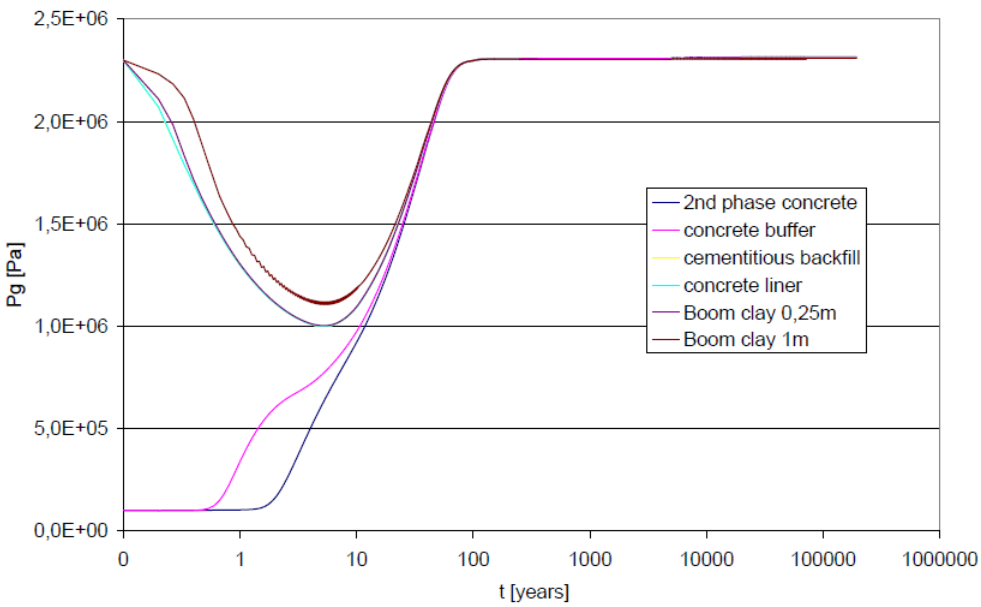

Figure 11: Gas pressure at different observation points as calculated by IRSN for the Supercontainer test case [26]

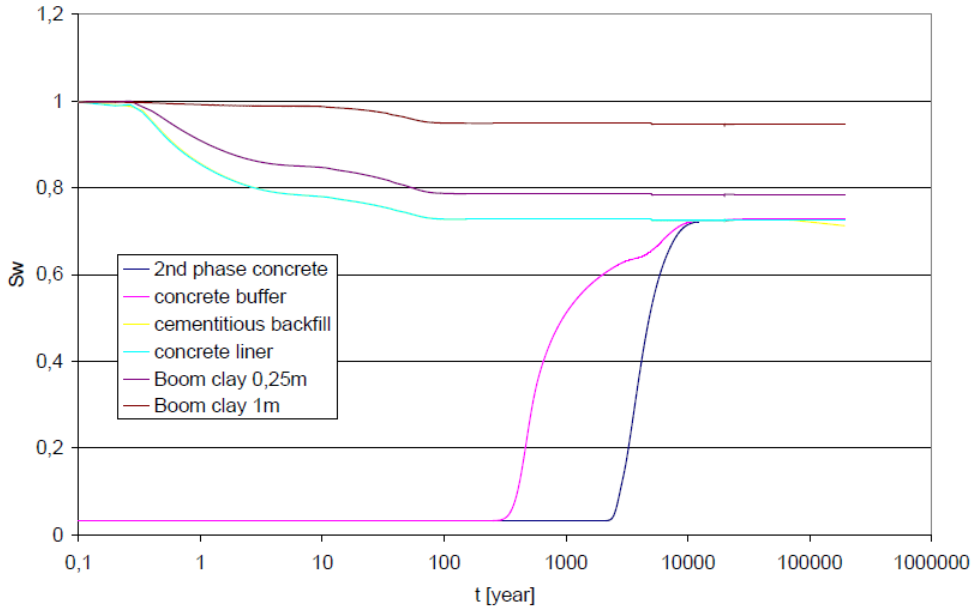

Figure 12: Water saturation at different observation points as calculated by IRSN for the Supercontainer test case [26]

As compared to the results obtained by CEA (Figure 10), in the axi-symmetrical model the rise of the gas pressure is quicker, but the maximal value in both cases was reached at the same time and is only slightly higher than the hydrostatic pressure. The relatively significant extend of the Boom Clay desaturation is also observed by CEA, however in CEA's results (Figure 10) the totality of the system resaturates much more rapidly. This may be due to the fact that in the axi-symmetrical model the surface of the outer boundary, participating to the masse exchange, is much larger than in the plane 2D model.

A comparison with the results of SCK·CEN is difficult, since SCK·CEN uses a gas generation term which is 10 times higher than the one given by the best estimate value of the corrosion rate, the basis of the source term used by CEA and IRSN. The kinetics of the system evolution is also influenced by fully saturated initial conditions that are applied in their study. SCK·CEN has taken into account gas dissolution in water and found that the maximal gas pressure reached in the system stayed on the same order of magnitude as the hydrostatic pressure. This indicates that the dissolution of hydrogen in water, which is known to be low, is nevertheless sufficient to counterbalance the higher gas production rate and the more restricted space available to gas because of the fully saturated conditions assumed by SCK·CEN.

3.2 Couplex-Gaz case

A system based on the Couplex-Gaz case [28, 41] was analysed by CEA [27] and IRSN [26]. This second test case was derived from the Couplex-Gaz benchmark proposed in 2006, based on Andra's concept for storage of intermediate level waste in a Callovo-Oxfordian clay [42].

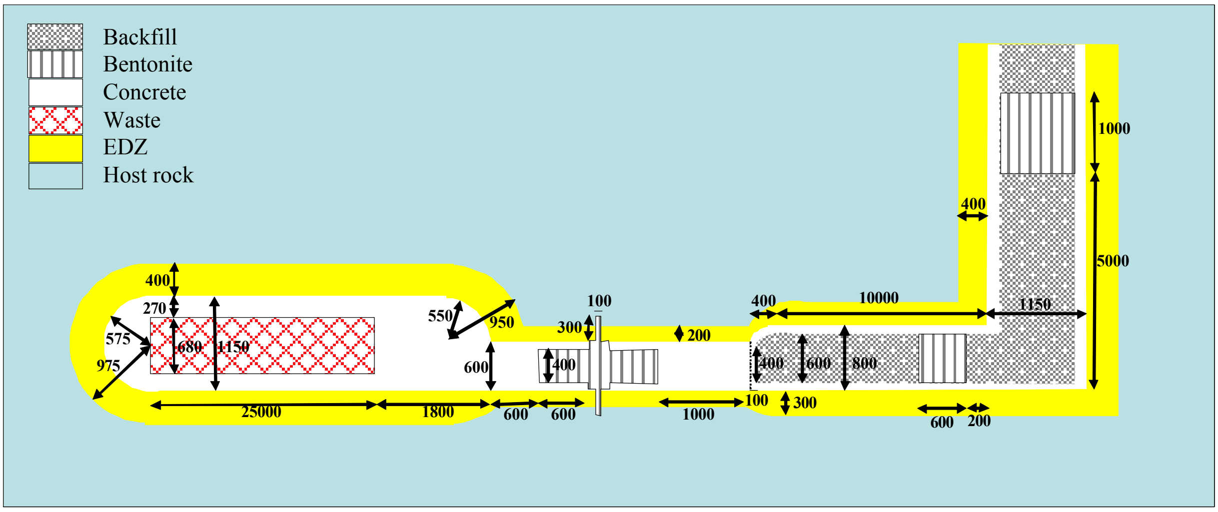

Figure 13: Geometry and dimensions (in cm) of the Couplex-Gaz benchmark case [26]

This original Couplex-Gaz test case presented a closed geometry with the vertical section of a disposal cell completely surrounded by the clay formation, which proved to limit the convective flows of both water and gas phases. In the present test case (Figure 13), a vertical section of a disposal cell together with a part of the access gallery and with the vertical shaft was chosen as an interesting variation of the original benchmark case. This configuration is supposed to be more realistic and allows addressing different transport regimes that may coexist. Figure 14 shows the model representation of this case in 2D, and Table 5 summarized the modelling parameter for the different model components. The time-dependent gas generation function is given in Figure 16. In the next two sections, the contributions of both partners are summarized.

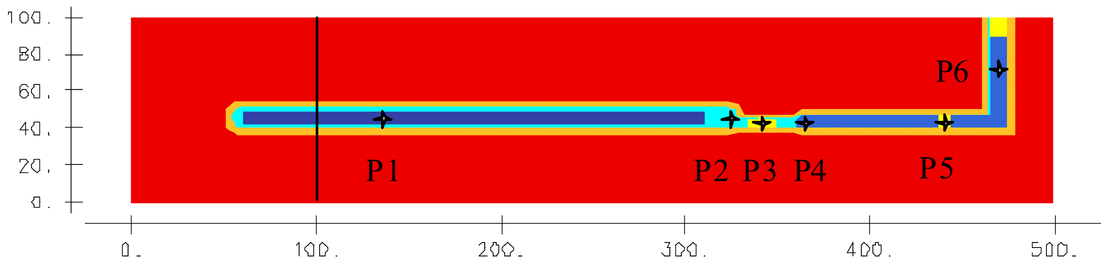

Figure 14: Model representation of the Couplex-Gaz benchmark case [26]

Table 5: Material parameters for the Couplex-Gaz case

parameter	waste package	concrete	bentonite	backfill	EDZ	clay
porosity ϕ [-]	0.25	0.15	0.35	0.35	0.15	0.15
permeability k [m^2]	$1.0 \cdot 10^{-15}$	$1.0 \cdot 10^{-19}$	$1.0 \cdot 10^{-20}$	$6.0 \cdot 10^{-16}$	$5.0 \cdot 10^{-18}$	$5.0 \cdot 10^{-20}$/ $5.0 \cdot 10^{-21}$*
van Genuchten parameter:						
shape parameter m [-]	0.33	0.35	0.38	0.30	0.33	0.33
residual liquid saturation S_{lr} [-]	0.01	0.01	0.01	0.01	0.2	0.4
residual gas saturation S_{gr} [-]	0	0	0	0	0	0
air entry pressure p_a [MPa]	0.03	2	16	0.6	5	15

* horizontal and vertical permeability, respectively

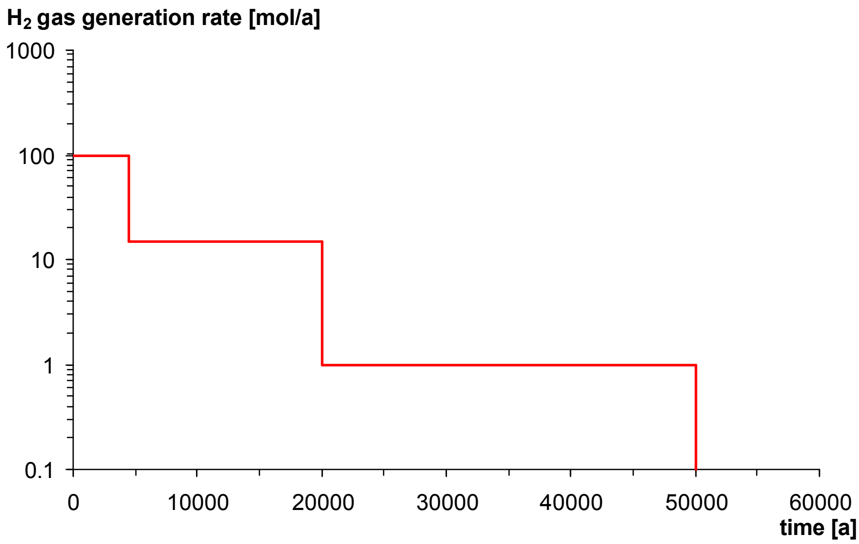

Figure 15: Evolution of the gas generation rate for the Couplex-Gaz case

3.2.1 CEA

The main objective of the CEA contribution [28] is to test the ability of two-phase flow codes to calculate time-dependent gas pressure and saturation evolution by using *Cast3m*, a two-phase flow code developed by CEA [39].

A two-phase flow calculation was performed, with the liquid phase and the solid matrix assumed to be incompressible. The relative permeabilities and capillary pressures are described by the van Genuchten model. For the model geometry and material properties see Table 5 and Figure 13. Modelling calculations are performed under isothermal conditions at T=289 K. The chosen boundary conditions are of *no flux* type on lateral vertical boundaries (left and right) and hydrostatic pressure on top and bottom boundaries (4.2 MPa on the top and 5.2 MPa on the bottom). Outside the waste package, CEA assumed fully saturated initial conditions, with a hydrostatic pressure of 4.2 MPa at the top border of the system. Inside the container, initially unsaturated conditions are supposed. For the initial gas pressure, CEA considering atmospheric pressure at the top boundary of the system, leading to a gas pressure of about 0.65 MPa inside the waste package. CEA did not account for the dissolution and diffusion of H_2 in the water phase (Table 1). For the evolution of gas generation see Figure 15.

Figure 16 shows the time dependent gas pressure on a vertical line through the repository. The lowest values are found in the waste (at about *0.55* at the x-axis). The saturation of the system is almost steady state, and a free gas phase only exists in the waste package area[1]. The gas pressure gradually increases with time because of the gas produced inside the waste.

Unfortunately, the fixed point algorithm CEA used for the calculation failed at time 360 years. For the longer term it is therefore not clear whether a gas breakthrough will occur.

Considering the short calculation time only reachable by CEA computations, the only two statements that can be done are:

- The key plug located at the entrance of the waste vault perfectly plays its role by avoiding gas migration toward the biosphere at early life time of the repository (before 350 years).
- The encountered numerical problems pointed out the possibility that classical numerical schemes/approaches can fail when dealing with two-phase flow simulation considering highly heterogeneous systems and sharp gas pressure/saturation fronts.

[1] note that the gas pressure values surrounding the waste area - where no gas exists - may be confusing from a physical point of view but the model needs it from a mathematical point of view

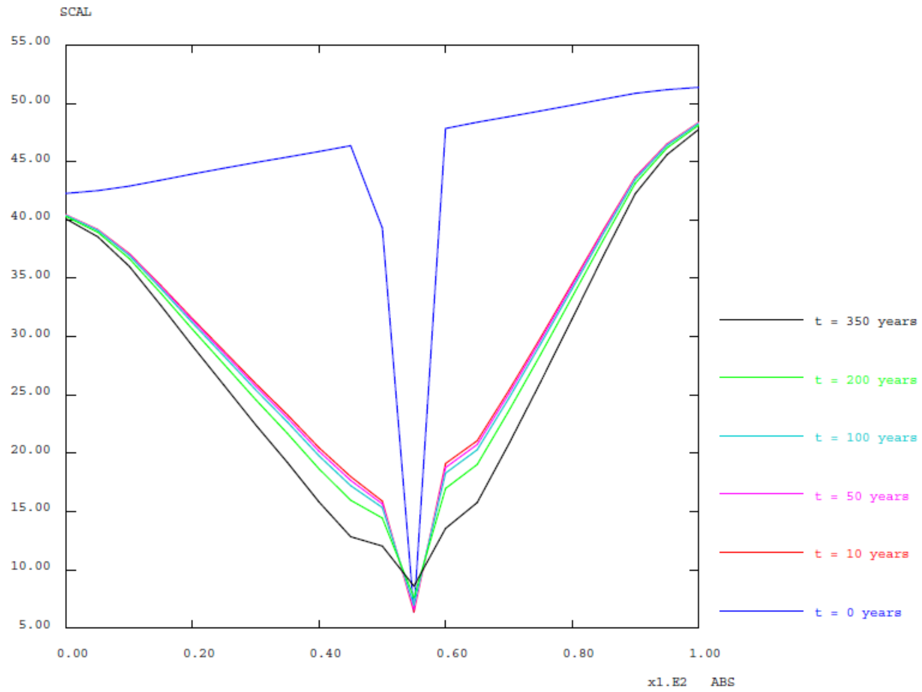

Figure 16: Gas pressure profiles (in 0.1 MPa) at times 0, 10, 50, 100, 200 and 350 years as calculated by CEA [27]. The x-axis represents a vertical line through the repository with the waste located at the pressure minimum

3.2.2 IRSN

The main goal of the contribution of IRSN [26] is the validation of the two-phase flow code *MiGasTra* [40] which they are developing. Next to the analysis of the Belgian Supercontainer concept discussed in Section 3.1.3, the Couplex-Gaz benchmark was used for a second test. The calculations are prepared together with CEA (see previous section) in order to compare the outcomes of the codes.

For the calculations, two-phase flow without dissolution and evaporation effects was considered, with the liquid phase and the solid matrix assumed to be incompressible, and the other phase follows the ideal gas law. For the model geometry and material properties see Table 5 and Figure 13. The mathematical model includes mass conservation laws for both one-component phases supplemented by generalized Darcy equations for each phase. The relative permeabilities and capillary pressure are described by the van Genuchten model. Due to the large geometric extensions of the Couplex-Gaz case, the effect of gravity was included. Outside the waste package, IRSN assumed fully saturated conditions; inside the container a reduced water saturation of 0.027 was assumed. For the evolution of the gas generation rate see Figure 15.

A triangular mesh of 1719 nodes (3334 elements) generated with *Cast3m* was used. With a very small time step (one order of magnitude lower then the one given by the implicit CFL condition) it was possible to obtain the convergence of the solver and the solution presented numerical characteristics consistent with the physical properties of the real variables. With a relatively coarse mesh it was possible to see the differences in saturation between different repository components (Figure 17). In this case the resaturation of the repository dominated and no gas overpressure (as compared to the hydrostatic pressure) was observed. This shows the importance of the choice of model geometry, since in the original Couplex-Gaz benchmark [28] an important increase of gas pressure (up to ~7 MPa) was observed. Another important quantity studied here was the time to reach the full resaturation of the repository. It has proved to be very long and was not reached in the simulations. In the original Couplex-Gaz case there was some dispersion of resaturation times between participants, but most of them were under 100’000 years. The enclosing host rock desaturated to a significant extent also in this test case (Figure 18), leading to a decreasing pressure in the compartment enclosing the waste (Figure 19).

The CEA results covering only the first 350 years, the host rock desaturation was very limited as well as in the majority of results of the Couplex-Gaz benchmark. Due to very low permeability of the clay and its steep capillary pressure curve, the relevant desaturation found on long distance is not expected to occur. This behaviour of the *MiGasTra* code may result from the numerical diffusion associated with upwinding (with respect to the flux direction) of the convection terms. In future work this point will be further investigated.

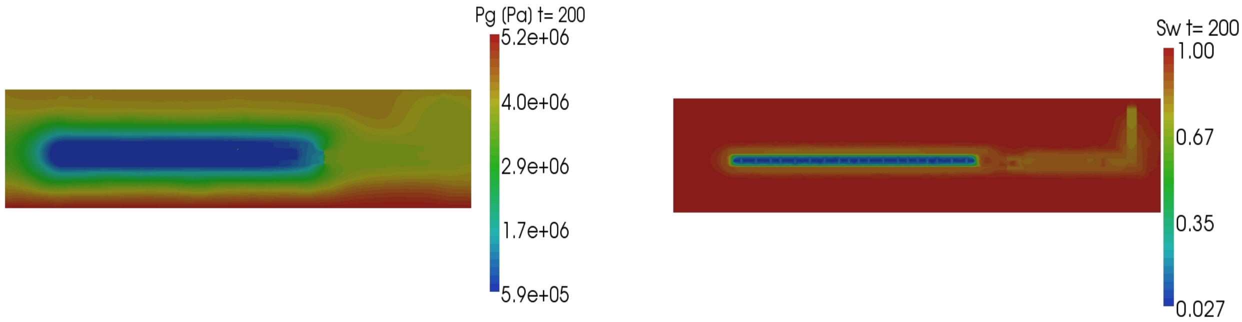

Figure 17: Gas pressure and water saturation maps at 200 years for the Couplex-Gaz test case as calculated by IRSN [26]

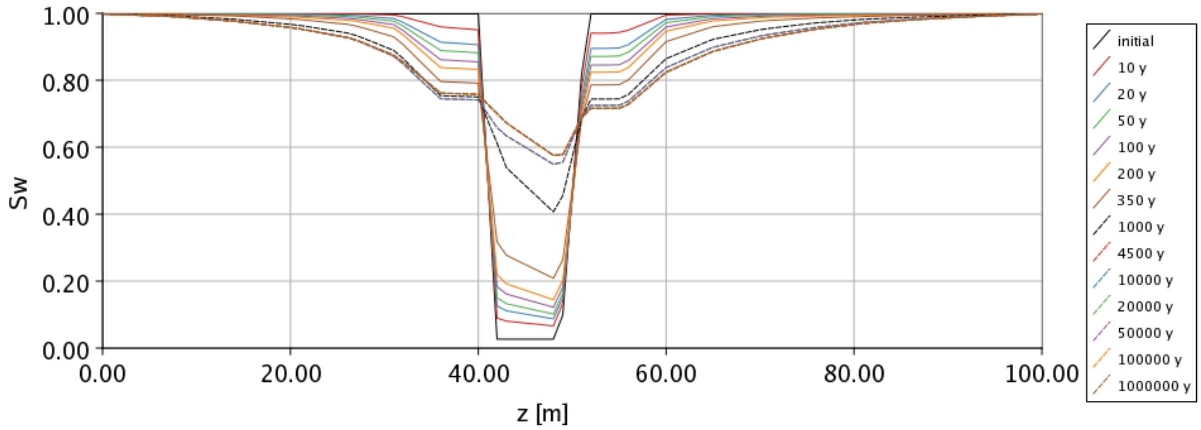

Figure 18: Saturation profiles along a vertical line crossing the storage cell (with the waste at about 45 m) as calculated for the Couplex-Gaz test case by IRSN [26]

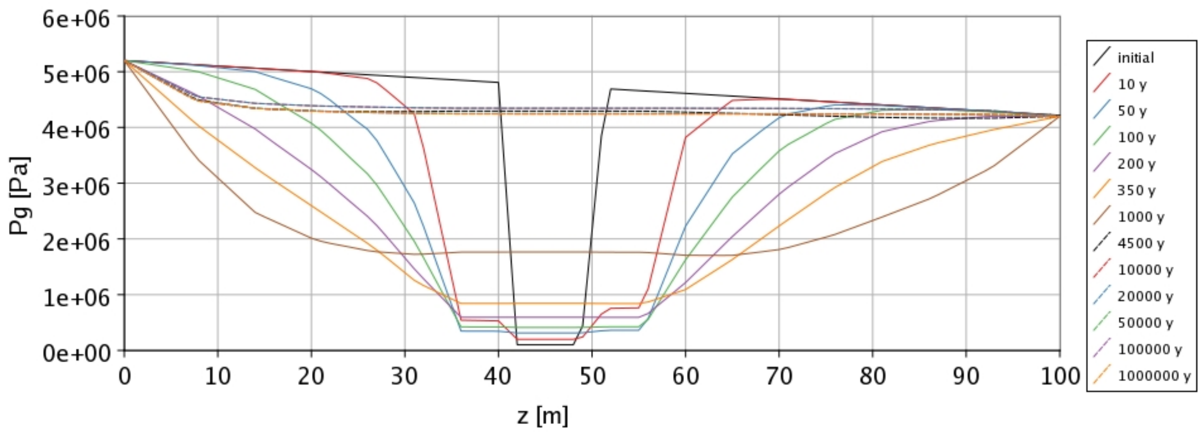

Figure 19: Gas pressure profiles along a vertical line crossing the storage cell (with the waste at about 45 m) as calculated for the Couplex-Gaz test case by IRSN [26]

3.3 Czech granite concept

NRI analyzed hydrogen generation and migration for the Czech concept of a deep geological repository for spent fuel in granite [30, 31]. A first estimation of NRI showed, that for their specific geometry diffusion is not sufficient to remove all H_2 gas generated by corrosion [30]. Therefore three different models simulating different gas transport situations were developed.

The first model, realized in the *GoldSim* environment [43], simulates transport of hydrogen from an intact container through the bentonite buffer and the further transport in host rock and other engineered barriers by diffusion only. A model representation of the Czech borehole concept (Figure 20) was realized as axi-symetrical 2D model. The two conservative gas generation scenarios used for this analysis are depicted in Figure 21.

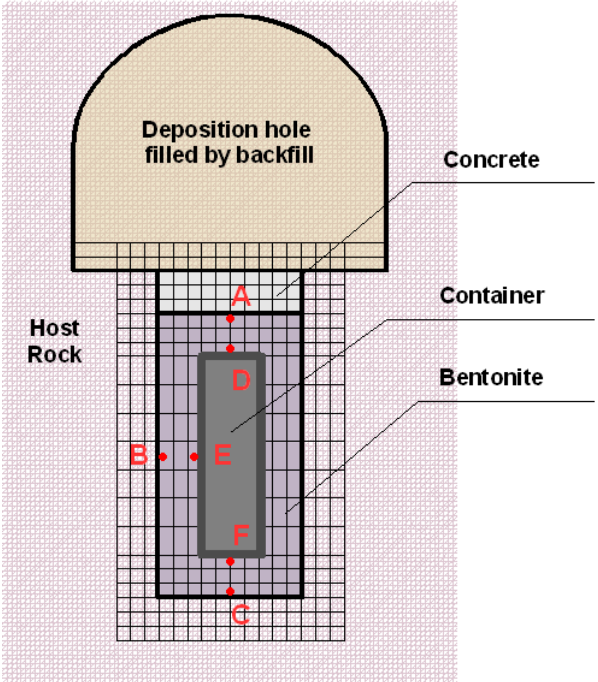

Figure 20: Model representation of the Czech borehole concept used for the first calculation [31]

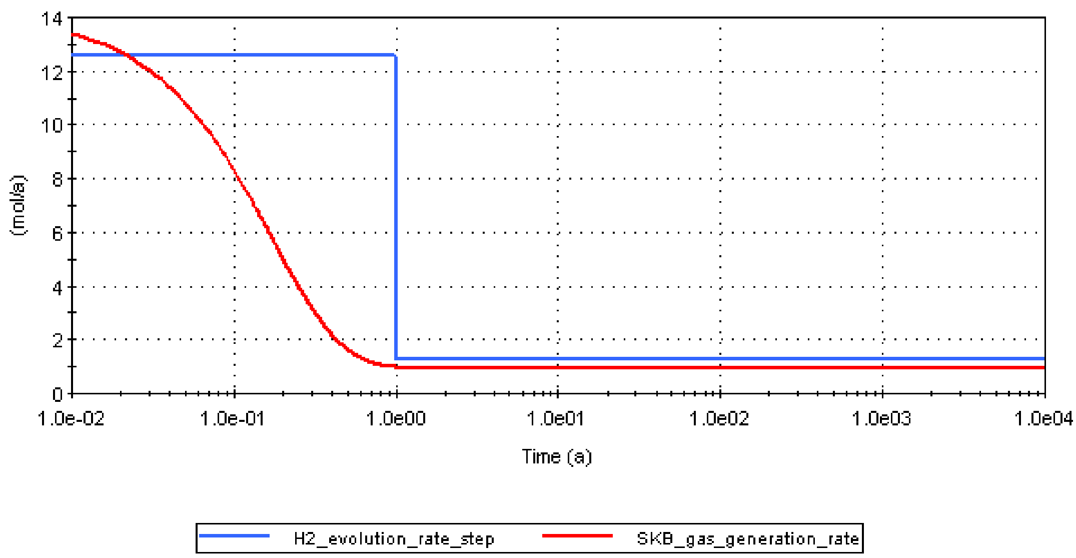

Figure 21: H_2 gas generation functions used for the Czech borehole concept [31]

The calculations showed that in case of the step function, gas migration by diffusion only is not sufficient to remove H_2 fast enough to avoid that the gas pressure will not exceed the gas entry pressure (10 MPa) of bentonite . (Figure 22).

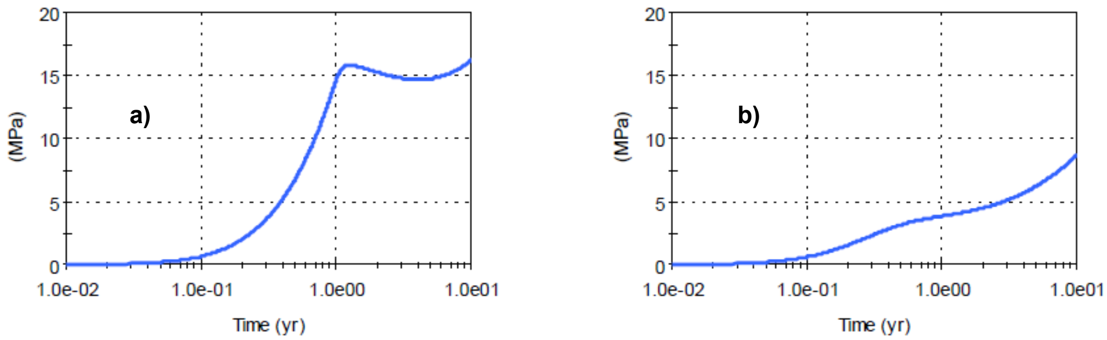

Figure 22: Evolution of gas pressure in the Czech borehole concept close to the waste container, assuming gas transport by diffusion only, for two gas generation scenario's: a) step function, b) exponential function [31]

The second model is a simplified 1D model used by NRI to understand the generalities of two-phase flow for the Czech borehole concept. It is realized in *TOUGH2* code [37], simulates two-phase flow from the intact container surface through the bentonite buffer. The model represents the 0.3 m thick and initially fully saturated bentonite layer enclosing the waste container surface. The material properties are summarized in Table 6. For the H_2 gas generation rate, a value of $1.6 \cdot 10^{-4}$ mol/a is used.

Table 6: Material parameters for the bentonite used in the Czech borehole concept

parameter	**bentonite**
porosity ϕ [-]	0.36
permeability k [m^2]	$6.0 \cdot 10^{-19}$
van Genuchten parameter:	
shape parameter m [-]	0.5
residual liquid saturation S_{lr} [-]	0.2
residual gas saturation S_{gr} [-]	0.01
air entry pressure p_a [MPa]	10

Figure 23 shows that the generated H_2 gas migrates slowly into the bentonite. To fill the whole bentonite buffer, it takes more than 150 years, and the resulting gas saturation of the bentonite buffer is less than 10%. The gas pressure stays below 10 MPa at all times.

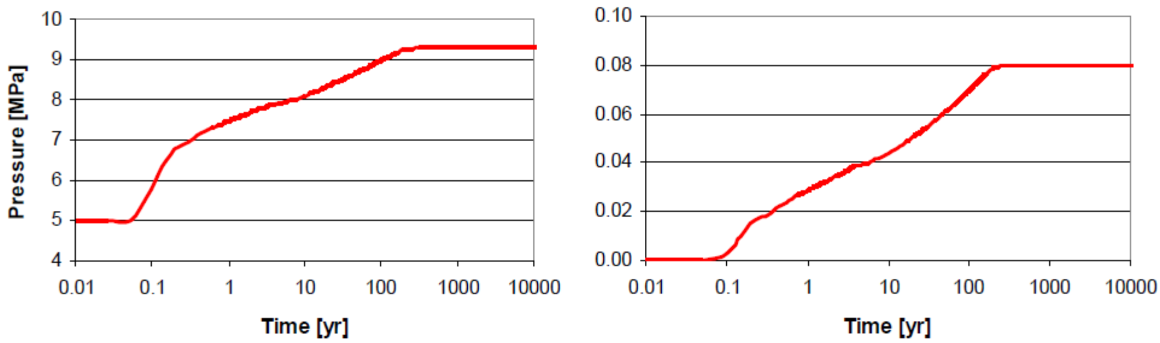

Figure 23: Evolution of gas pressure and gas saturation close to the waste container surface in the Czech borehole concept for the second calculation [31]

In the third model, NRI simulates gas migration in the borehole in the event of a container cracking, when water fills the container and H_2 gas generation will increase. A 2D axi-symetrical model of the borehole (Figure 24), calculating isothermal two-phase flow at 35°C, was realized in *TOUGH2* [37].

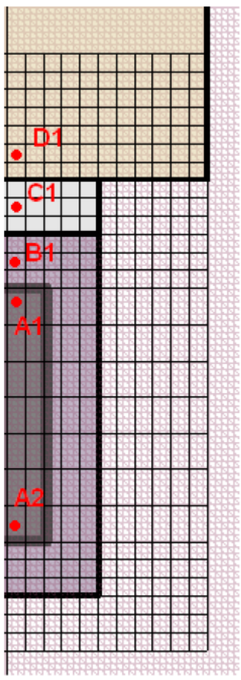

Figure 24: Model representation of the Czech borehole concept used for the third calculation [31] . See also Figure 20.

For this model calculation, NRI used a very conservative gas generation rate of 223 mol/a to represent the increased (short term) gas generation after container failure. Gas generation is equally distributed over the waste, assuming a porosity of 0.2 and a permeability of 10^{-14} m^2. The bentonite properties are summarized in Table 6. Because corrosion process is assumed to have taken place already over a long period at the moment the container fails, an initial gas saturation of 0.2 is assumed (hydrostatic pressure 5 MPa).

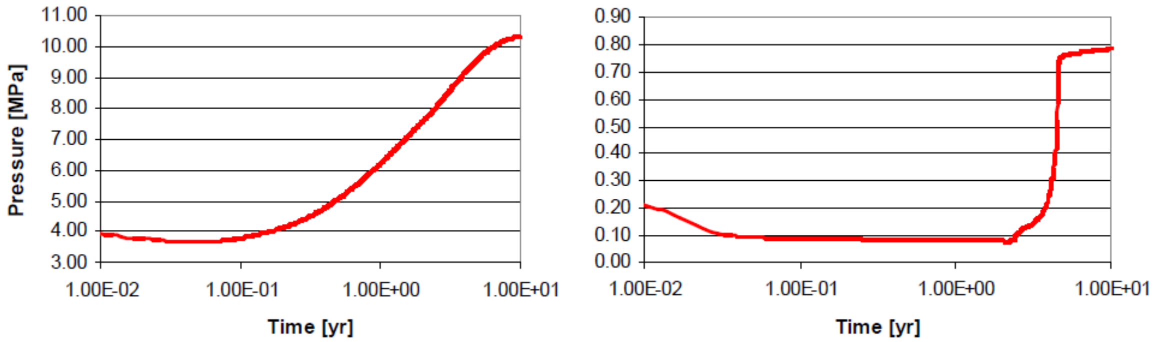

Figure 25: Evolution of gas pressure and gas saturation at the top of the waste container in the Czech borehole concept for the third calculation [31]

Figure 25 shows the evolution of the gas pressure at the top of the container in the first ten years after container failure. The pressure does not exceed 11 MPa at this point or anywhere else in the bentonite. The gas saturation is below 0.85, but it is assumed by NRI, that this will not slow down the corrosion process, since sufficient water is still present at the container surface.

3.4 German hypothetical clay concept

GRS developed a conceptual model for pathway dilation and implemented this into the two-phase flow code *TOUGH2* [37] to account for dilation effects [17, 29]. The modified code was used to investigate the influence of pathway dilation on the far-field transport of gas generated in a hypothetical German repository for radioactive wastes in clay stone, and to identify sensitive parameters.

The conceptual model to describe this effect used by GRS is summarised in the next section, followed by a condensed description how this conceptual model is represented in the two-phase-flow code *TOUGH2* [2]. The third section addresses the repository system analysed by GRS and summarizes the calculation results.

[2] for a more elaborated description of the implementation of pathway dilation processes by GRS see [17, 29]

Conceptual model

When the entry of gas is regulated by capillary forces, a gas phase will first enter the largest pores of a saturated clay and thus dilation will first affect these pores. Postulating that dilation tends to locate at pores which are already dilated, only a small pore fraction will be subjected to pathway dilation. These dilating pores are partially filled with water. The conceptual model assumes that this water, which only presents a very small amount of the water content of the clay, is supposed to be irrelevant in terms of liquid phase and gas phase flow and in terms of capillary pressure.

The original porosity in the non-dilated state will be called *primary porosity* in the following, whereas the porosity gained by dilation will be called *secondary porosity*. It has to be noted that dilated pores contribute to both, primary and secondary porosity. However, the pore fraction that belongs to the primary porosity is supposed to be of minor relevance for the flow processes for the mentioned reasons.

The present state of the conceptual model does not address hydro-mechanical interaction between dilated and non-dilated pores, because these are assumed not to be significant.

The consequence of the assumptions is that water will be present only in the primary porosity and will not “see” any dilation effects. Capillary pressures thus remain constant in relation to the water content and water flow will be enhanced by the pressure of the intruding gas phase but not by dilation of water filled pores. Experimental data indeed indicate that the amount of water displaced by creation of additional gas pathways is very small for both, bentonite [44] and natural clays [6]. In the proposed model the gas phase is expected to be able to flow through the clay without needing to displace water, i.e. it will be able to move even if the pore water is completely immobile (which might e.g. be forced by boundary conditions).

It is assumed that dilation processes are fast in relation to the pressure build up (quick equilibration of pressure and porosity) and that there aren’t any memory effects. It shall be possible to describe flows at element scale by Darcy's law (no intermittent gas flow), which implies that a homogeneous representation of dilation effects must be possible. It is assumed that the hydraulic effects of pathway dilation can be described adequately by a pressure-dependent porosity and a pressure-dependent anisotropic gas permeability.

The assumed quick equilibration implies that the propagation of the front of the dilation zone does not show any kinetic effects and does not give any resistance to the flow of the gas phase. This means that the dilation front is “soft” and can propagate easily through the rock as long as there is sufficient gas supply. This assumption probably does not apply to salt rock, where a pressure-dependent front velocity can be observed (on experimental time-scales).

Model implementation

A pressure-dependent porosity need to be introduced into the code *TOUGH2*/*EOS7* in order to create additional storage capacity for the gas phase that allows the gas phase to flow without needing to displace water. The increase of porosity was modelled independently from the *porosity-change* feature of *TOUGH2* because this feature affects the fluxes but not the pore volume. Since each porosity change affects the local physical state (in terms of liquid saturation, capillary pressure, pressure and density of the liquid and gas phase, pressure and density of gas phase, water density, vapour density, density of dissolved H_2, and internal energy) the state change during expansion or compression of the pore space was calculated by the thermodynamic processes implemented in the used *EOS7*-module.

A simplified model for the anisotropy of the gas phase flux due to dilation was introduced by defining a set of micro-crack networks, each with its own dilation threshold, anisotropic permeability-pressure relationship, and porosity-pressure relationship.

The *TOUGH2* equation for the gas phase flow F_{gas} was redefined by adding a term describing the sum of the gas phase fluxes in n micro-crack networks

$$F_{\mathrm{gas}} = -\left(\underbrace{\frac{\rho_{\mathrm{gas}}}{\mu_{\mathrm{gas}}} k\, k_{\mathrm{r,gas}} \mathbf{I}}_{\substack{\text{determines the gas flux}\\ \text{in the primary porosity}}} + \underbrace{\frac{\rho_{\mathrm{gas}}}{\mu_{\mathrm{gas}}} \sum_{i=1}^{n} \mathbf{K}_{\mathrm{dil},\,i} k_{\mathrm{dil},\,i}(p_{\mathrm{gas}})}_{\substack{\text{determines the gas flux in the secondary}\\ \text{porosity of } n \text{ micro-crack networks}}} \right)(\nabla p_{\mathrm{gas}} - \rho_{\mathrm{gas}} g) \qquad \text{Eq. 11}$$

where k is the absolute and $k_{\mathrm{r,gas}}$ the relative gas permeability, ρ_{gas} the density, μ_{gas} the dynamic viscosity of the gas phase, and g the vector of gravitational acceleration. $k_{\mathrm{dil},\,i}$ is the pressure-dependent gas permeability of micro-crack network i and tensor $\mathbf{K}_{\mathrm{dil},\,i}$ is introduced in order to make gas permeability dependent on flow direction.

There are several possibilities to introduce a pressure-dependency of the gas flux e.g. by defining a pressure-dependent relative gas-permeability or intrinsic permeability. Modelling the gas flux through the primary and secondary porosity independently, as it was done here implies that these fluxes are quite independent as proposed in the conceptual model. This approach also allows a decoupling of weighting schemes for the flow in dilated and non-dilated pores. By defining an upwind weighting scheme for the gas flux in the secondary porosity the intended easy propagation of the dilation front according to the assumption of quick equilibration can be achieved.

For $k_{\mathrm{dil},\,i}$ the exponential relationship Eq. 12

$$k_{\mathrm{dil},\,i}(p_{\mathrm{g}}) \stackrel{\mathrm{def}}{=} \begin{cases} 0 & \text{for} \quad p_{\mathrm{g}} \le p_{\mathrm{thr},i} \\ \left(\dfrac{p_{\mathrm{g}} - p_{\mathrm{thr},\,i}}{\Delta p}\right)^{\alpha} \Delta k_{\mathrm{dil},\,i} & \text{for} \quad p_{\mathrm{g}} > p_{\mathrm{thr},i} \end{cases} \qquad \text{Eq. 12}$$

was used, where $\alpha > 1$ is an arbitrary exponent and Δp defines a pressure interval [$p_{\mathrm{thr},i}$, $p_{\mathrm{thr},i} + \Delta p$] over which gas permeability changes by $\Delta k_{\mathrm{dil},\,i}$.

The porosity ϕ is defined as the sum of the initial porosity ϕ_0 and the porosity of each micro-crack network ϕ_i:

$$\phi = \phi_0 + \sum_{i=1}^{n} \phi_i(p_{\mathrm{g}}) \qquad \text{Eq. 13}$$

Assuming that micro-cracks are parallel plates which open according to a linear elastic law a linear *"dilation relationship"* between crack porosity ϕ_i and gas pressure

$$\phi_i(p_{\mathrm{g}}) \stackrel{\mathrm{def}}{=} \begin{cases} 0 & \text{for} \quad p_{\mathrm{g}} \le p_{\mathrm{thr},i} \\ \dfrac{p_{\mathrm{g}} - p_{\mathrm{thr},i}}{\Delta p} \Delta\phi & \text{for} \quad p_{\mathrm{g}} > p_{\mathrm{thr},i} \end{cases} \qquad \text{Eq. 14}$$

is postulated. Here, p_{g} is the gas pressure, and p_{thr} a threshold pressure for the onset of dilation. Δp defines a pressure interval [$p_{\mathrm{thr},i}$, $p_{\mathrm{thr},i}+\Delta p$] over which porosity changes by $\Delta\phi$. Other, e.g. non-linear, dilation relationships may be defined by the user with the obligation that porosity increases monotonously with pressure.

Due to the strong non-linearity of the relationships describing the dilation behaviour, porosity and permeability are changed after completion of a time step in order to avoid convergence problems. The automatic time stepping procedure provided by *TOUGH2* has been modified in order to simulate the dilation-controlled transport processes appropriately.

Modelling of hypothetical clay repository

For the hypothetical clay repository, GRS defined a rectangular model domain representing a horizontal clay layer which is confined by aquifers to the top and to the bottom (Figure 26).

The model represents one quarter of the repository; the domain's height is 430 m, its lateral length is 2500 m by 1500 m or 4000 m by 3000 m depending on the considered simulation case.

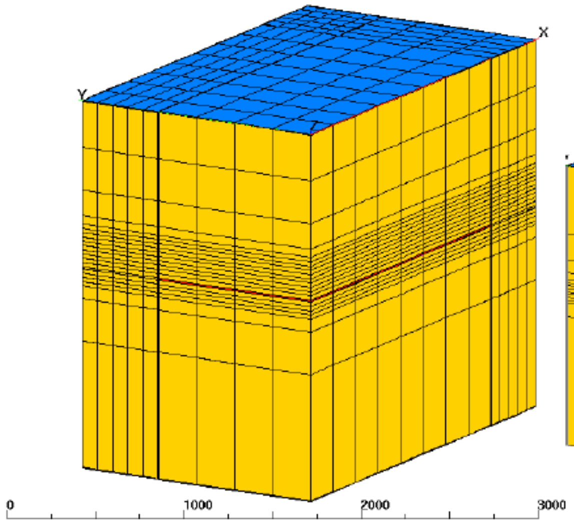

Figure 26: Two model representation of the German hypothetical clay concept [17]

The repository is located at a depth of 450 m and 190 m below the upper boundary of the computational domain in a vertical edge of the domain with lateral lengths of 1 km by 2 km. All lateral boundaries are no-flow boundaries, either being far away boundaries or symmetry planes. At the top and to the bottom, fixed pressure boundaries are used (aquifers). All simulations start with an equilibrated hydraulic state. GRS used a modified van Genuchten function were p_c does not fall below p_{entry} except for very low gas saturation levels, where it is assumed that p_c drops linearly to 0. A reference case and 16 additional cases where defined in which one or two model parameters were varied against the reference case to identify sensitive parameters. The parameterization of the reference case is summarized in Table 7; parameterizations for the other calculation cases can be found in [17]. The H_2 gas generation rate for the total repository system is depicted in Figure 27.

Table 7: Material parameters for the German hypothetical clay concept (reference case) [17]

parameter	clay	repository
porosity ϕ [-]	0.1	0.0
lateral permeability $k_{x,y}$ [m^2]	$3.3 \cdot 10^{-21}$	$1.0 \cdot 10^{-18}$
vertical permeability k_z [m^2]	$6.6 \cdot 10^{-22}$	$1.0 \cdot 10^{-18}$
van Genuchten parameter:		
shape parameter m [-]	0.43	-
residual liquid saturation S_{lr} [-]	0.1	-
residual gas saturation S_{gr} [-]	0.02	-
air entry pressure p_a [MPa]	7.56*	-
pathway dilation threshold pressure p_{thr} [MPa]	0.76 σ_{min}**	-

* *modified van Genuchten expression*

** σ_{min}: *minimal principal stress (see [17])*

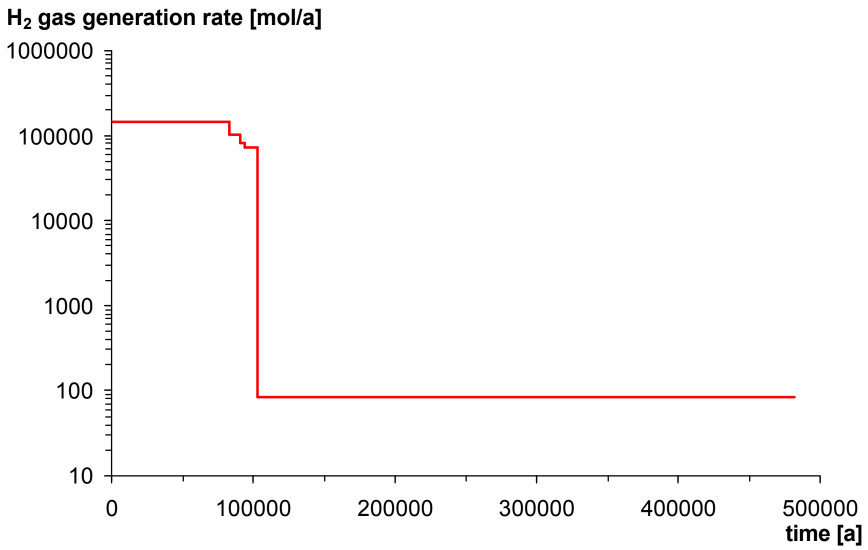

Figure 27: Evolution of the gas generation rate for the German hypothetical clay case

Figure 28 shows the extent of the dilation zone (‘*secondary porosity*’) for the reference case (*Ref*) and cases with several degrees of anisotropy of the permeability (the cases *Iso*, *HiAniso*, and *2D* are equal to a lateral/vertical anisotropy of 1, 0.1, 0.001, and 0, respectively). The cases *Ref* and *Iso* do not show any lateral propagation of the gas phase. There is a relatively slight horizontal propagation of the gas phase in case *HiAniso* but the vertical movement of the gas phase is predominant. Only in case *2D* where the vertical gas permeability of the secondary pore space is set to zero, the horizontal propagation of the gas phase exceeds the vertical propagation. The distribution of the secondary porosity which displays the propagation of the dilation zone is quite similar (Figure 28). It has to be noted that the lateral extent of the dilation zone probably depends on the height of the repository which is 2.5 m in all cases.

The fact that a strong anisotropy of the gas permeability is needed to achieve a horizontal propagation of the dilation zone can be explained by the depth-dependency of the minimal principal stress. In case of an upward propagation of the front, these thresholds decrease continuously since they are linearly dependent on the minimal principal stress. In case of a horizontal propagation of the dilation front the dilation thresholds remain constant.

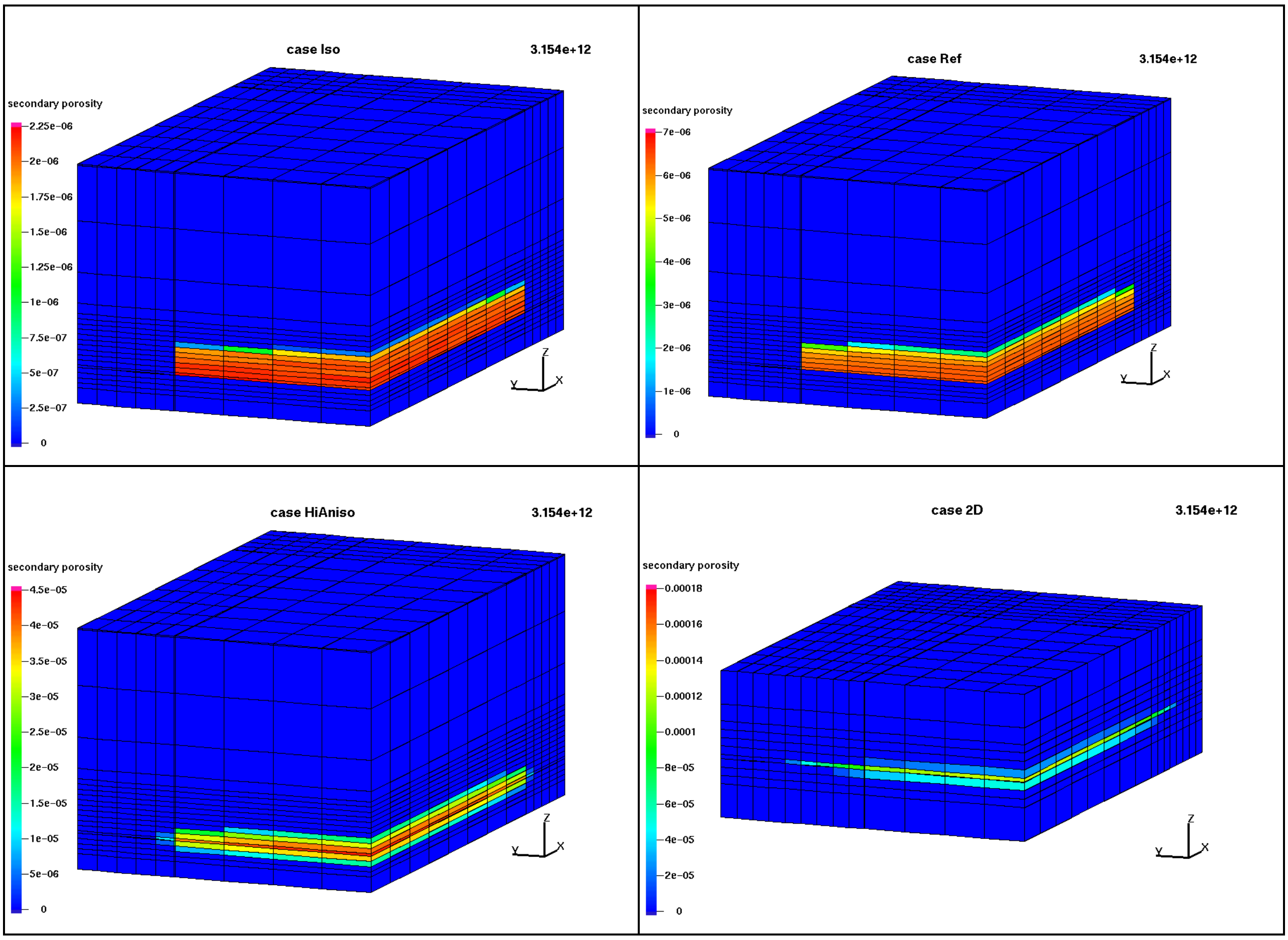

Figure 28: Secondary porosity in the vicinity of the repository as calculated by GRS [17].The z-axis is exaggerated by a factor of 5.

Figure 29 shows the evolution of the gas pressure inside the repository for the period from 0 years to 200’00 years for the reference case and all other calculation cases. For comparison, the threshold pressure for dilation and macro-fracturing at repository depth is depicted in this figure, too (9.3 MPa and 12.3 MPa, respectively).

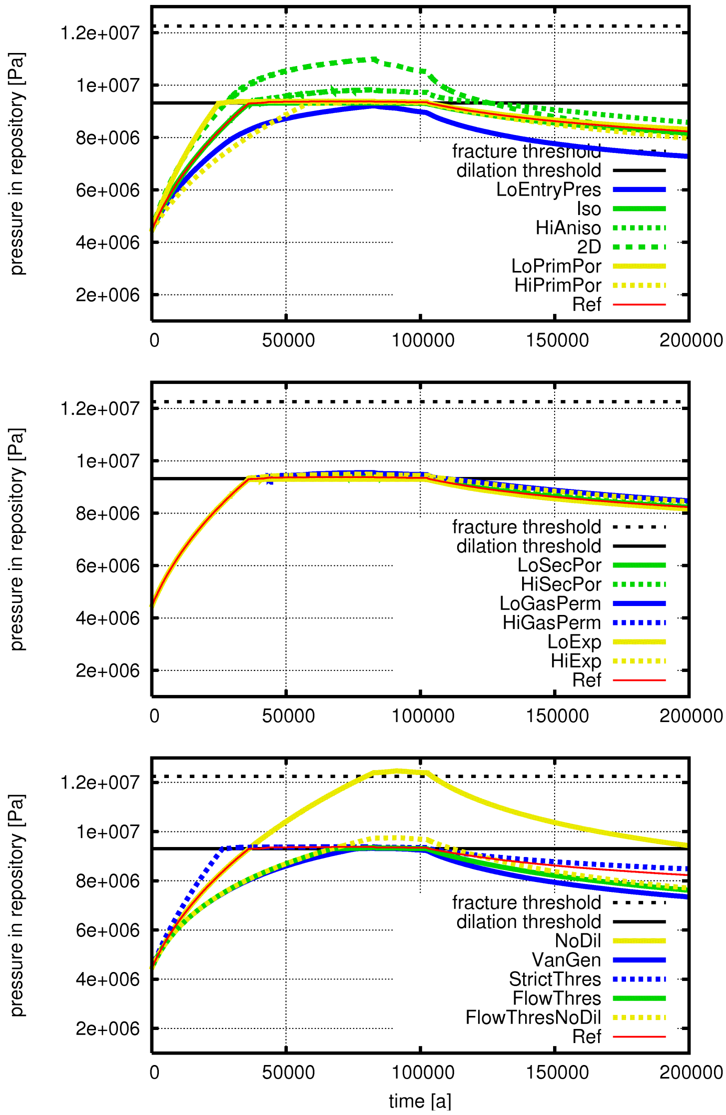

Figure 29: Pressure evolution in the German hypothetical clay repository as calculated by GRS [17]. The solid and dotted horizontal lines are the fracture and dilation thresholds at repository depth, respectively.

In all cases with pathway dilation, gas pressure in the repository stays below the dilation threshold up to year 2500 and from year 12’700 on. Maximum pressures are reached at about 90’000 years. Macro-fracturing takes place only in case *NoDil* which does not account for dilation effects (Figure 29 bottom). In all other calculation cases, no macro-fracturing is found, indicating that the process of pathway-dilation efficiently inhibits the evolution of macro-fractures. No dilation takes place if the gas entry pressure is as low as 2.16 MPa (*LoEntryPres*), i.e. that the gas pressure at the point of gas entry ($p_{hyd}+p_{entry}$ = 4.41 MPa) is below the dilation threshold (9.31 MPa).

The maximum pressure which is observed in the repository increases with decreasing isotropy and decreasing primary porosity. It also increases if a modified van Genuchten function is used, i.e. if capillary pressures rise more quickly in the course of desaturation. An increase of isotropy (*Iso*) in relation to the reference case has only minor effect on the pressure evolution inside the repository. This also applies to the specific pressure-dependency of the gas permeability (*LoGasPerm*, *HiGasPerm*, *LoExp*, *HiExp*) and of the secondary porosity (*LoSecPor*, *HiSecPor*).

The extent of the dilation zone can be quantified by the volume of dilated grid elements representing host rock. The results show that the maximum volume of the dilation zone increases with

- increasing isotropy of the gas permeability,
- decreasing primary porosity, and
- a more rapid increase of capillary pressures during desaturation.

Apparently, the maximum volume of the dilation zone has the same sensitive parameters as the pressure evolution inside the repository.

H_2 is stored either in dissolved or gaseous form. Because water is present only in the primary porosity according to the conceptual model, there are three H_2-fractions to distinguish:

- Dissolved H_2 in the primary porosity,
- Gaseous H_2 in the primary porosity, and
- Gaseous H_2 in the secondary porosity.

In all cases the relative amount of H_2 in the secondary porosity was very small (10^2 to 10^4 times smaller than the gaseous fraction in the primary porosity) which attributes to the very small porosity increase due to dilation. Thus, the gas phase is predominantly stored in the primary porosity. It can be concluded from this that the capillary pressures, which have immediate influence on desaturation, have a stronger effect on the storage capacity of the rock for a gas phase than the porosity increase due to dilation.

For the considered generic repository model it was found that the dilation process facilitates the escape of gas from the repository considerably. This leads to an effective limitation of gas pressures inside the repository and prevents macro-fracturing in cases where the advective flow of gas in the primary porosity is very small.

The dilation threshold, the capillary pressure function, the anisotropy of pressure-induced gas permeability, and the primary porosity have the strongest impact on the pressure limitation and on the volume of the dilated rock zone. The life time of the dilation zone is mainly affected by the gas generation rate and the amount of dilation.

The specific pressure-dependency of the gas permeability and secondary porosity above the dilation thresholds has no major influence on the gas migration process. The corresponding parameters are therefore judged to be not sensitive for the considered reference case. This is beneficial for the safety assessment with regard to the uncertainties connected to the experimental quantification of these parameters.

4. Discussion

Four different repository systems were analysed by the five partners of WP3.2 and a summary of the results was given in the previous chapter. One of the main objectives of all contributions to WP3.2 is to quantify the balance between gas generation and gas migration, and to compute the resulting gas pressure in the different repository components. Table 8 summarizes the maximum gas pressure calculated and compares it with the gas entry pressures defined for the various materials in the case studies.

Table 8: Apparent gas entry pressure p_r^{vG} and calculated maximum gas pressure p_g for the different repository concepts and components

case	**material**	**calculated maximum gas pressure** p_g **[MPa]**	**gas entry pressure** p_r^{vG} **[MPa]**
Belgian Supercontainer concept	2nd phase concrete	2.3 - 3.2	0.5
	buffer	2.3 - 3.0	0.5
	backfill	2.3 - 2.4	0.5
	lining	2.3	0.5
	Boom Clay	2.2-2.3	2.8
Couplex-Gaz case	waste package	4.4	0.03
	concrete	4.8	2.0
	bentonite	4.8	16
	backfill	4.8	0.6
	EDZ	±2.5	5.0
	clay	5.2	15
Czech granite concept	bentonite	10 (11#)	10
German hypothetical clay concept	clay	10*	7.6**/9.3***

n.d. not determined
\# *damaged container case*
* *except for case without pathway dilation*
** *modified van Genuchten expression*
*** *dilation threshold*

By comparing the gas entry pressures with the calculated maximum gas pressures, it can be derived which compartments are (temporary) desaturated by intruding H_2 gas. However, as discussed in Section 2.2.3, different definitions of the term '*gas entry pressure*' are available:

- the *capillary pressure* or *actual gas entry pressure* p_c is the pressure difference between gas pressure and hydrostatic pressure
- the *apparent gas entry pressure* p_r^{vG} is a parameter of the Van Genuchten model.

Table 8 refers to the van Genuchten (apparent) gas entry pressure p_r^{vG}. It should be noted, that in the van Genuchten model a distribution of pore sizes is assumed. Gas will therefore enter the porous medium through the widest pores first, where the capillary effect and other water retention effects are negligible. Thus, some gas will enter the porous medium already before the apparent gas entry pressure p_r^{vG} is exceeded, i.e. when the gas pressure exceeds the hydrostatic pressure. However, Table 8 shows that for the Supercontainer case and the Couplex-Gaz case the EBS provides a volume that is relatively easy accessible for gas. The results of the calculations in both cases suggests that the EBS is sufficiently large to contain all free gas at approximately hydrostatic pressure, and no two-phase flow develops in the host rock for these cases. For the NRI case, two-phase flow develops in the bentonite (EBS) that shields the canisters from the groundwater in the granite host rock. For the GRS case, the gas migrates through the clay host rock by pathway dilation.

4.1 Potential safety issues

As stated before, the contributions of the different partners have different scopes varying from implementation of new process models, testing of numerical calculation schemes, analyses of generic test cases to (preliminary) analyses of potential safety issues. From the safety aspects summarized in Section 2.1, not all are therefore addressed in WP3.2.

Table 9 gives an overview on the potential safety aspects addressed in this work package. Generally, in this work package all partners focussed in their contributions on the analysis of pressure dependent safety aspects and therefore not perform any analysis of radionuclides migration, either soluble or gaseous. The issues of *gas driven nuclide migration* and *migration of radioactive gases* are thus not addressed in this work package.[3] Potential safety issues connected to *flammability hazard* are not analysed, too.

[3] for a contribution to the issue of migration of radioactive gases we refer to WP2.2 [14]

Table 9: Treatment of potential safety issues in WP3.2 ('-': not treated, '(+)': partially treated, '+': treated)

potential safety issue	CEA	GRS	IRSN	NRI	SCK·CEN
gas driven nuclide migration	-	-	-	-	-
migration of radioactive gases	-	-	-	-	-
overpressurization	(+)	+	(+)	(+)	+
retarded resaturation	(+)	-	(+)	(+)	(+)
thermal properties of the system	-	-	-	(+)	(+)
flammability hazard	-	-	-	-	-

Overpressurization

In Table 8, the calculated maximum pressure for the different materials and calculation cases are summarized. In case of the Supercontainer, SCK·CEN stated, that at the calculated - relatively low - maximum pressures macro-fracturing of the concrete is assumed to be unlikely. Although CEA and IRSN does not give a statement on this question, their calculated gas pressures are consistent with the results of SCK·CEN. Overpressurization was not addressed in the analyses of the Couplex-Gaz case. NRI recognizes the potential issue of overpressurization and discussed it in [45]. NRI found during supportive experimental work performed within WP3.2 [30], that bentonite samples can lose integrity after several breakthroughs. However, due to the approximate character of their modelling work, no conclusion was given from NRI with regard to the likelihood of overpressurization effects for the Czech granite concept. For the hypothetical clay concept analysed by GRS, it has been shown that for all parameterizations analysed, overpressurization is not appearing as long as the process of pathway dilation is accounted for in the model (Figure 29).

Retarded resaturation

The previous chapter has shown for the considered disposal concepts that free gas can develop in the EBS close to the metal surfaces. All partners calculated the gas saturation within the different materials, but did not perform mechanical stress analyses due to the swelling of clay or bentonite barriers. In all contributions to WP3.2, complete resaturation does not appear within the calculated time interval (CEA: 320’000 years[4], GRS: 500’000 years, IRSN: 100’000 years[4]/1’000’000 years[5], NRI: 10’000 years, SCK·CEN: 3000 years/100’000 years in an additional benchmark calculation [24]). Consequently, safety issues connected to resaturation, e.g. changes in stress conditions in case of swelling clays and their consequences are not discussed by any of the partners.

Thermal properties of the system

Thermal aspects are addressed explicitly by NRI and SCK·CEN. CEA, GRS and IRSN performed isothermal calculations. SCK·CEN analysed the influence of temperature on several processes, e.g. H_2 generation, H_2 solubility and diffusion, but did not discuss the influences of gas generation and migration on the heat conductivity of these materials explicitly. However, desaturation is limited in all cases (<30% [24]) and may therefore limit the influence of gas on the thermal properties of the system. NRI analysed and discussed the appearance of gas bubbles at the container surface, but their main interest is the influence of the gas bubbles on the corrosion rate. However, in principle their consideration may also serve to estimate the impact on the temperature distribution around the heat emitting HLW.

4.2 Modelling of gas migration processes

Reliable models and tools are available to model the migration of gas via dissolution and subsequent diffusion or advective transport by Darcy two-phase flow, making use of the van Genuchten approach. This has already been recognized in EVEGAS, MEGAS, and PEGASUS [7, 8, 9]. Although the codes used by the partners have their specific limitations, these processes are addressed with sufficient robustness by all partners. However, the contribution of CEA (Section 3.2.1) shows that sharp saturation/pressure fronts in complex model geometries can induce numerical problems that may raise the need for new spatial schemes to analyse this particular systems.

The processes of diffusion, two-phase flow, pathway dilation and overpressurization are assumed to be sequential processes that gain their relevance with increasing pressure. Since these processes are also of increasing complexity, the most rational way to address the migration of H_2 gas generated by the corrosion of the waste packages is to analyse first, if dissolution and diffusion of H_2 in the water phase is sufficient to remove the generated gas. Diffusion is a well understood process, and is relatively easy to analyse and to implement in a computer code. For the calculation of diffusion processes, only a few parameters are necessary, i.e. the material porosity and the apparent diffusion constant are the most

[4] Supercontainer case
[5] Couplex-Gaz case

important. Furthermore, both constants can be derived experimentally with adequate precision.

SCK·CEN performed an analysis based on diffusion only as the first step for the Supercontainer concept (Section 3.1.1) and concluded that for the conservative assumptions made, gas migration by diffusion may temporarily have insufficient capacity to prevent an increase of the pressure in the EBS. However, more advanced analyses show that beyond the EBS, in the Boom Clay host rock, diffusion processes have sufficient capacity to remove the generated H_2 gas. In contrast, a first analysis by NRI for the Czech granite concept (Section 3.3) showed that for this concept gas removal by diffusion is insufficient and two-phase flow has to be considered.

For the application of two-phase flow models, uncertainties are not only present about the parameterization of the van Genuchten model, but also on the general use of Darcy-based models for clay materials [3]. However, the analyses of the Supercontainer concept (Section 3.1), the Couplex-Gaz case (Section 3.2) and the Czech repository concept (Section 3.3) has shown that two-phase flow has in principle the potential to decrease gas pressure sufficiently. SCK·CEN made an detailed analysis of the impact of heat generation on two-phase flow processes and found that the influence on the gas generation can be substantial, but the overall influence on the gas transport was small [24]. NRI pointed out that the formation of gas bubbles may locally inhibit the corrosion of the waste container, but found this effect difficult to quantify [30]. The achievements within this work package have shown that the tools to analyse two-phase flow are thought adequate, but the challenging task of proving that the (conceptual) models used are comprehensive still remains. Substantial efforts are still necessary in the domains of model qualification and, if possible, validation. In this respect, much is expected from the recently started EU-FP7 FORGE project [13], in which the various models for the gas generation and migration will be benchmarked to experiments and in which process level knowledge will be further developed.

In case of the application of the pathway dilation process, the uncertainty is even larger. “Classical” two-phase flow models with static pore space are not well suitable for cases where the gas transport is significantly controlled by deformation processes affecting the pore space. The migration of gas via self-created and stress-induced pathways is more difficult to model, but GRS presented a conceptual model for pathway dilation and proposed a way to implement this model into the two-phase flow code *TOUGH2* (Section 3.4). Ideally, the local stress field should be considered along with a realistic constitutive model of the mechanical behaviour of the host rock, but it is not clear whether this is really necessary. Although qualitative understanding of the processes involved is available, the step to quantitative modelling is complicated by a lack of accepted microphysical and mechanical models and tools that adequately describe the response of saturated clay to increased gas pressure.

The conceptual model calculations performed by GRS may give a good general insight in the relevant parameters and the capacity of pathway dilation to prevent overpressurization, but experimental evidence for this process and its actual implementation is still insufficient. Furthermore, the results achieved by GRS might not be transferable to other repository concepts or site properties, especially if repository depth, gas generation rates, two-phase flow properties and dilation properties differ significantly. Many assumptions of the considered case are subject to uncertainty or might be a too strong simplification of reality: homogeneity has been assumed for the initial conditions and for the properties of the host rock, and the process of resaturation has not been considered for the definition of initial conditions and gas generation rates. There is also considerable uncertainty regarding the two-phase properties of the clay at high liquid saturations. In order to substantiate the conceptual model description of pathway dilation by GRS, experimental evidence is needed regarding the anisotropy of pathway dilation in clay stone and the two-phase flow properties of clay for high liquid saturations. Additional consideration of mechanical interactions between stress field, flow and dilation processes might prove necessary in the future.

Alternatively, unaltered conventional two-phase flow models with adapted parameterizations may be used for the calculations of pathway dilation facilitated gas transport. Based on sufficient experimental data, a proper parameterization may be derived that fit in common two-phase codes. Principally, two quantities needs calibration by experiments: (1) the capillary pressure function that is used to introduce a gas entry pressure (together with the relative gas permeability) and (2) the flow rate that is possible when the gas phase is able to flow through the rock.

Although the conditions that leads to the formation of macro-fractures have not been considered in the present work package, all studies indicates that the gas pressure will be lower than or of the same order of magnitude as the lithostatic pressure, at least if pathway dilation is considered (Table 8). The occurrence of macro-fractures, even if it is unlikely and never observed in representative experimental conditions, surely is still an important safety related question connected to gas migration. The main safety concern is: in case macro-fractures may form, will these represent a long-lasting pathway for potential radionuclide migration? Experiments and qualitative arguments have been assembled that demonstrate that a crack is not necessary a long-lasting radionuclide migration pathway due to the self-sealing capability of the clay [46]. However, a safety concept which has to rely on self-sealing has to cope with considerable uncertainties in the safety assessment due to the complexity of self-healing processes and due to possible multi-scale structures generated by macro-fractures.

The safety-assessment can thus be simplified significantly if the absence of macro-fracturing can be demonstrated with sufficient confidence. To determine the maximum gas pressure, it is necessary to improve the basis for the modelling of the gas migration by two-phase flow and stress-induced pathway dilations. Because no conclusive model description of these pressure induced deformation processes are available at the present, the gas migration models addressing this overpressurization effects have a significant empirical component and must therefore be calibrated and validated by experiments (a topic currently addressed in the EC-FP7 FORGE project [13]).

5. Conclusions

From the analyses of the role of gas generation and migration on the repository performance as carried out in WP3.2, the following general sequence of processes can be derived:

- Due to chemical processes, H_2 gas will be generated on the surface of steel components in the repository as soon as anaerobic conditions are present and the surface comes into contact with water

- The gas generation rate may be low, but due to the long term corrosion of all iron containing components, relevant amounts of H_2 gas can be formed

- After the first contact with water and after cracking of a container, gas generation can be temporarily increased

- A significant amount of the generated gas will be removed from the local gas sources by dissolution and diffusion in the water phase

- When the capacity of diffusion process is insufficient to remove the generated gas, gas pressure will build up

- The appearance of gas bubbles on the steel surfaces may decrease the corrosion rate

- When the gas entry pressure of the enclosing material is exceeded, two-phase flow may happen, removing the gas more efficiently from the source than diffusion only. The pore volumes of the materials surrounding the waste containers will then partly be filled with (non-dissolved) gas. Two-phase flow will appear earlier in concrete-based materials than in clays

- Pathway dilation may appear and increase the capacity of gas removal by two-phase flow

- If the gas removal capacity is still insufficient and the pressure increases further, overpressurization may happen (although no indication that gas pressure will rise that much is found in the present work package)

From the potential safety aspects summarized in Section 2.1, this work package focussed on the balance between gas generation and gas migration. Although no critical stress conditions were defined, for the systems considered in the present work package it is not likely to assume overpressurization to happen, because even without assuming pathway dilation, the maximum gas pressures found (Table 8) were around the order of magnitude of the lithostatic pressure.

No attempt is made within this work package to quantify the pressure-induced migration of gaseous or dissolved radionuclides and the influence of gas volumes on the dissipation of heat from the HLW. Because an assessment of these potential safety issues is based on the same processes as addressed in this work package, all considerations and model developments discussed in the previous paragraphs are also relevant to analyse these safety aspects.

As pointed out in the previous chapter, the tools to analyse two-phase flow are adequate, but substantial efforts are still necessary in the domains of model qualification and validation. The models and assumptions that have been used in the present work package still need a better understanding on process scale. However, the analyses performed in this work package gives useful information on the relevance of the different processes on repository safety that need to be focussed on in future research.

Appendix A Summary of the contribution of CEA

Milestone M3.2.3

CEA conducted some two-phase flow computations on the Belgian super-container concept test case described in Milestone M3.2.1 and M3.2.4 in order to test the ability of the two-phase flow code developed by CEA in the *Cast3m* environment.

Calculation results indicate that total saturation of the system takes about 320'000 years. Saturation front propagates from the initial saturated area toward the inner part of the system. Gas pressure evolution in the system is faster than water pressure and reached equilibrium in less than 5'000 years. Gas overpressure inside second phase concrete and concrete buffer then occurs and peaks at 40'000 years before to disappear.

If the gas source term due to the waste overpack seems to delay the total saturation of the second phase concrete and the concrete buffer and to create a transient gas overpressure inside those materials, no clear impact of gas source term linked to the liner was shown. Some additional computations conducted without this "liner" source term presented some very close results except for the gas pressure build-up presenting a faster evolution taking into account the "liner" source term. Those results point out the influence of the source term location assumptions.

Some small saturation oscillations as well as small pressure oscillations are obtained in our computations. Those small numerical artefacts can provide from our choice of time step evolution (geometric progression) that lead to regular time step cuttings in order to reach a fast fixed point algorithm convergence (less than 20 iterations) but can also stems from the use of non regular hexahedrons mesh cells. Those points need additional investigations.

Milestone M3.2.10

CEA conducted some two-phase flow computations on the two dimensional B waste Couplex-Gaz concept test case #2 described in Milestone M3.2.1 and M3.2.4 in order to test the ability of the two-phase flow code developed by CEA in the *Cast3m* environment

CEA encountered some numerical problems in the fixed point algorithm and were not able to conduct the computation until the full saturation of the system. Depending on the convergence criteria value chosen and on the time step evolution strategy, fixed point algorithm failure can be off two different types but always occurs around the same calculation time. For the first type of failure, the convergence criteria value was never reached inducing the decreasing of the calculation time step towards very low value without any change. For the second type of failure, increasing oscillations inside the fixed point algorithm evolution lead to the convergence criteria occurrence inducing pressure gas decrease toward non physical zero value inside the waste package area. As CEA do not face this problem for test case #1 (see milestone M3.2.3), even if small numerical artefacts were encountered, furthermore investigations are necessary in order to solve the problem. At this stage, the main differences between calculation case #1 and case #2 are first the type of mesh cells used and second the higher level of heterogeneity exhibited by case #2.

Until the failure of the fixed point algorithm at time 360 years, the results obtained were in agreement with a possible evolution of the unsaturated repository system.

Saturation of the system is almost steady state with a waste package area remaining at the same unsaturated level as the gas produced inside the wastes increase the gas pressure. Due to the use of our classical two-phase flow model, gas pressure propagates quickly inside the system even if no gas exists outside the waste package area. This allows to check the high efficiency of the saturated bentonite key plug to contain gas inside the waste package area and to avoid gas propagation to connecting drift and shaft backfill

Appendix B Summary of the contribution of GRS

The code *TOUGH2/EOS7* has been modified to account for the mechanism of pathway dilation in clay stones with very low permeability [17]. This code was named *TOUGH2-PD* (*TOUGH2* with pathway dilation). A pressure-dependent porosity has been introduced in order to allow a gas phase to flow without need to displace the liquid phase. Whether desaturation and water displacement takes place or not is strongly influenced by the constitutive two-phase flow relations which are used. The *TOUGH2-PD* code does not exclude displacement of water by the gas phase but it is able to handle cases where such a displacement is difficult e.g. due to no-flow boundary conditions or very rigorous gas entry thresholds.

Porosity increase was modelled separately from the porosity-change-feature of *TOUGH2* which affects the fluxes but not the storage capacity of the rock. Gas permeability was defined by adding a pressure-dependent gas flux within the secondary porosity (created by dilation) to the gas flux in the primary porosity. Liquid permeability is not affected by the dilation process because the dilated pore space is thought to be created and used mainly by the gas phase. This also aims at reproducing the observation of low water displacement in gas migration experiments. The approach of separate gas fluxes in the primary and secondary pore space also allows decoupling of weighting schemes for these two flows and thus a realisation of the intended easy propagation of the dilation front according to the assumption of quick equilibration.

The modified *TOUGH2* code has been applied to a hypothetical German repository for radioactive waste with non-negligible heat generation (heat transport was not simulated). In 17 alternative cases, one or two model parameters were varied against a reference case to identify sensitive parameters.

For the considered generic repository model it was found that the dilation process facilitates the escape of gas from the repository considerably. This leads to an effective limitation of gas pressures inside the repository and prevents macro-fracturing in cases where the advective flow of gas in the primary porosity is very small.

Sensitive Parameters

The dilation threshold, the capillary pressure function, the anisotropy of pressure-induced gas permeability, and the primary porosity have the strongest impact on the pressure limitation and on the volume of the dilated rock zone. The life time of the dilation zone is mainly affected by the gas generation rate and the amount of dilation.

The specific pressure-dependency of the gas permeability and secondary porosity above the dilation thresholds has no major influence on the gas migration process. The corresponding parameters are therefore judged to be not sensitive for the considered reference case. This is beneficial for the safety assessment with regard to the uncertainties connected to the experimental quantification of these parameters.

Possibly the influence of the specific pressure-dependency of the gas permeability and secondary porosity was overruled by the dominant influence of the dilation threshold decrease in upward direction. Therefore, the choice of dilation parameters might still be of importance in systems with constant dilation thresholds, e.g. in systems with horizontal propagation of the dilation zone or in small-scale systems.

Geometry of the dilation zone

In the model, a strong anisotropy of the dilation-induced gas permeability is needed to force the dilation zone to propagate in the horizontal instead of the vertical direction (bedding planes are thought to be orientated horizontally). This attributes to the fact that the minimal principal stresses decrease in upward direction. The dilation thresholds, which are connected to the minimal principal stress, therefore continuously drop at the dilation front as it moves upward through the host rock. This facilitates the propagation of the dilation zone and furthermore decreases the gas pressures inside the repository. Therefore, from the viewpoint of safety, a vertical propagation of the dilation zone is more favourable than a horizontal one.

Still, clay stone has a strong textural and mechanical anisotropy which facilitates a gas flow parallel to the bedding planes. It has to be investigated by experiments whether the mechanical anisotropy of clay stone is large enough to force a horizontal propagation of the dilation zone along the bedding planes or whether a vertical propagation will take place.

It has to be noted that in the observed case of a vanishing vertical component of the additional gas flux caused by dilation (for extreme anisotropy), gas migration and pressure evolution will probably depend on the thickness of the clay layer which is subjected to dilation. The thickness of this layer does not need to correspond with the height of the repository. An estimation of this thickness is probably connected to large uncertainties.

Storage Capacity for the Gas Phase

The gas migration shows a strong dependency on the host rock's storage capacity for a gas phase. The main factors controlling the storage capacity are the primary porosity and the capillary pressure function. In all considered cases, the secondary porosity gained by dilation was too small to have a significant influence on the storage capacity for a gas phase. Thus, desaturation of the primary porosity was the driving process for the storage of the gas phase. However, it has to be noted that this observation strongly depends on the capillary pressure functions that have been used. If one would assume a very rigorous threshold behaviour for gas entry into a saturated clay stone and a dilation threshold lower than the gas entry threshold there would not be any desaturation of the primary porosity and the gas phase would be stored only in the secondary porosity.

Gas Entry Pressures and Capillary Pressure Function

The importance of the capillary pressure function implies that gas migration reacts sensitively to the way gas entry pressures are introduced. As explained in Section 5.2.6, p. 43 [17], different relative gas permeability and capillary pressure functions can be used to introduce the same gas entry pressure. Yet, different capillary pressure functions allow different amounts of desaturation and imply different storage capacities for the gas phase. It has to be concluded that the constitutive two-phase flow relations for the capillary pressure and relative gas permeability do not only have to reflect the gas entry behaviour of the rock correctly but also have to capture the storage capacity of the rock for the gas phase. This requires accurate experimental measurements of capillary pressures at the high liquid saturations which can be expected under repository conditions in order to quantify how much desaturation is possible during the flow of the gas phase.

When desaturating the rock, the commonly used van Genuchten capillary pressure function shows an increase of the capillary pressure which is relatively slow compared to what could be expected for clay stone. The van Genuchten function might therefore overestimate the storage capacity for the gas phase and consequently underestimate the gas pressures inside the repository. The van Genuchten function, which is a quite common standard assumption, should therefore be treated with care in the context of gas migration in clay stone.

Transferability and Outlook

The results achieved in this study depend on the definition of the reference case and might not be transferable to other repository concepts or site properties, especially if repository depth, gas generation rates, two-phase flow properties and dilation properties differ significantly. Many assumptions of the considered reference case are subject to uncertainty or might be a too strong simplification of reality. Homogeneity has been assumed for the initial conditions and for the properties of the host rock. The process of resaturation of the host rock has not been considered for the definition of initial conditions and gas generation rates, which are dependent on water availability for metal corrosion. There is considerable uncertainty regarding the two-phase properties of the clay at high liquid saturations, especially with regard to the storage capability of the primary pore space for a gas phase. This storage capability might still be overestimated in the considered calculation cases. A decrease would increase the importance of gas storage in secondary pore space.

In order to substantiate the findings of this study, experimental evidence is needed regarding the anisotropy of pathway dilation in clay stone and the two-phase flow properties of clay for high liquid saturations. The proposed model still has to be qualified with respect to the physical relevance of the conceptual model. Additional consideration of mechanical interactions between stress field, flow and dilation processes might prove necessary in the future.

Appendix C Summary of the contribution of IRSN

The test cases and benchmark calculations proposed in PAMINA WP3.2 were considered by IRSN as an interesting framework for completing the validation of the two-phase flow code called *MiGasTra* that was under development in IRSN. Most of the work that has been done consisted in choosing and implementing an efficient numerical scheme in 2D which should be easily upgradeable from 2D to 3D. IRSN's stating point was a global pressure model, where a new unphysical variable of global pressure is introduced. This allows decoupling the system of two equations, and thus it is much easier to solve the problem. However, the global pressure approach presents two requirements that are not met in the case of hydrogen migration in clays. These requirements are the exponential gas law and a homogeneous capillary pressure law (one rock model). How to redefine in an optimal way the global pressure for the case with an ideal gas law and with multiple capillary pressure curves is still an open question. This situation was the motivation to change the approach and to use a conventional gas pressure – water saturation formulation. Keeping in mind the efficiency requirement, a vertex centred finite volume scheme on an arbitrary triangular mesh has been implemented. IRSN has then tested the code on a 2D case of the Andra's Couplex-Gaz benchmark (contribution submitted in January 2008).

The *MiGasTra* code simulates a two-phase flow without dissolution and evaporation effects. The liquid phase and the solid matrix are assumed incompressible, and the gas phase follows the ideal gas law. The starting point is the mass conservation laws for both one-component phases supplemented by generalized Darcy equations for each phase. The van Genuchten model is used for the relative permeability and capillary pressure. After some algebra the set of coupled non-linear diffusion-convection equations for water saturation S and gas pressure p is obtained:

$$\Phi \frac{\partial \boldsymbol{S}}{\partial \boldsymbol{t}} + \boldsymbol{div}(\boldsymbol{f}_w(\boldsymbol{S})\vec{\boldsymbol{q}}) + \boldsymbol{div}(\boldsymbol{K}\nabla\alpha_2(\boldsymbol{S})) + \boldsymbol{div}(\overline{\lambda}(\boldsymbol{S})(\rho - \boldsymbol{A}(\boldsymbol{p})\boldsymbol{K}\vec{\boldsymbol{g}})) = \frac{\boldsymbol{Q}_w}{\rho} \tag{1}$$

$$\Phi \frac{\partial}{\partial \boldsymbol{t}}\big(\boldsymbol{S}(\rho - \boldsymbol{A}(\boldsymbol{p})) + \boldsymbol{A}(\boldsymbol{p})\big) + \boldsymbol{div}(\boldsymbol{G}_1(\boldsymbol{S},\boldsymbol{p})\boldsymbol{K}\nabla\boldsymbol{p}) + \boldsymbol{div}(\rho\boldsymbol{K}\nabla\alpha_1(\boldsymbol{S})) + \boldsymbol{div}(\boldsymbol{G}_2(\boldsymbol{S},\boldsymbol{p})\boldsymbol{K}\vec{\boldsymbol{g}})) = \boldsymbol{Q}_w + \boldsymbol{Q}_g \tag{2}$$

where the nonlinear functions of p and S are defined as follows:

$$G_1(S,p) = A(p)\lambda_g + \rho\lambda_w$$
$$G_2(S,p) = \left(A(p)\right)^2\lambda_g + \rho^2\lambda_w$$
$$\alpha_1(S) = -\int_S^1 \lambda_w(s)P_c^{'}(s)ds$$
$$\alpha_2(S) = -\int_S^1 \overline{\lambda}(s)P_c^{'}(s)ds$$
$$\vec{q} = \vec{q}_g + \vec{q}_w = -\lambda(S)K\nabla p + K\nabla\alpha_1(S) + \rho G_1(S,p)K\vec{g}$$

$$\lambda_\alpha(S) = \frac{k_{r\alpha}}{\mu_\alpha}, \quad \lambda(S) = \lambda_g(S) + \lambda_w(S), \quad \overline{\lambda}(S) = \frac{\lambda_g(S)\lambda_w(S)}{\lambda(S)}$$

and $A(p)=\rho_g$ is the gas law which can be of any type, but we use the ideal gas law.

The finite element P^1 method is used for diffusion type terms and finite volume vertex centered Godunov scheme for convective type terms. An upwinding strategy is applied to the two convection terms using the arithmetic means on the pressure values inside each element. The convection term arising from the gravity contribution contains a non-monotone function and therefore simple upwinding is not adequate. It can be done, for example, with 1D Godunov scheme. The CFL condition on the length of the time step arising with explicitly solved convection terms was avoided by the sequentially implicit time discretisation. Being given S^n and p^n, the field velocity $\vec{q}^{\,n}$ is calculated by piecewise linear conforming triangular finite elements. Then the couple (S^{n+1}, p^{n+1}) is calculated by solving equations (1-2) sequentially. The fixed point method is for the resolution of the nonlinear equations.

A special attention has been paid to the treatment of the saturation S and of the capillary pressure p_c on the interfaces between different materials. Since all the pressures are supposed to be continuous (mechanical equilibrium state), the saturation can be discontinuous if both materials have different capillary pressure curves. Given S_j on the interface between materials having different capillary pressure curves, it is possible to reconstruct two (or more) saturations corresponding to the elements belonging to the control volume of the vertex j. We use an approach based on homogenization which allows mass conservation on the interface and is compatible with existence of residual saturations.

Two calculation test cases were defined together with CEA. The first one was based on the same geometry as the one proposed by SCK·CEN in Milestone 3.2.1 [47]. In contrast with the original case, the hydrogen dissolution in water and water evaporation were neglected. Only isothermal conditions were modelled and the water phase as well as the solid phase was considered as incompressible. The Supercontainer steel envelopes are seen as "phantom", which means that no specific transfer barriers are associated with them. First results obtained with this test case correspond to calculations made in 2D plane geometry, where the surface density of gas production was kept the same as in the original case. A second difference consisted in putting to zero of all the residual saturations. The overall behaviour of the system was found to be very similar to that obtained by CEA: the gas production is too weak to prevent the resaturation of the disposal cell and the maximal gas pressure (2.35 MPa) is just above the hydrostatic pressure.

The second test case was inspired by the Couplex-Gaz benchmark from Andra proposed in 2006. This exercise was based on Andra's concept for HAVL disposal in the Callovo-Oxfordian clay. The 2D benchmark test cases presented a closed geometry with the vertical section of a disposal cell completely surrounded by the clay formation, which proved to limit the convective flows of both water and gas. The dominant transport regime was diffusive in all parts of the repository and thus the efficiency of numerical treatment of the convective terms was impossible to check. Furthermore, the time necessary to dissipate the whole amount of hydrogen was found to be very long (~10^5 years). For this reason, IRSN proposed to study a vertical section of a disposal cell together with a part of the access gallery and with the vertical shaft. This configuration is supposed to be more realistic and allows to address different transport regimes that may coexist. The EDZ around the gallery connects the hydrogen production site with the vertical shaft, thus allowing a quicker gas evacuation. The simulation domain dimensions are 500 m horizontally and 100 m vertically. In this test, gravity is included. The model includes six materials with properties taken from the Couplex-Gaz. However, the rather complex geometry of this case is difficult to represent with a good quality mesh even in 2D. Up to now, the simulations were made on triangular meshes, which are not fulfilling completely the Delaunay criteria. The simulations were made for up to 100'000 years. With a very small time step (one order of magnitude lower then the one given by the CFL condition) it was possible to obtain the convergence of the solver and the solution presented numerical characteristics consistent with the physical properties of the real variables. With a relatively coarse mesh it was possible to see the differences in saturation between different repository components. In this case only the resaturation of the repository dominated and no gas overpressure (as compared to the hydrostatic pressure) was observed. This shows the importance of the choice of model geometry, since in the original Andra's Couplex-Gaz benchmark a significant increase of gas pressure (up to ~7 MPa) was observed. Another important magnitude was the time to reach the full resaturation of the repository. It has proved to be very long and was not reached in the simulations. In the Andra's Couplex-Gaz there was some dispersion of resaturation times between participants, but most of them were under 100'000 years. The host rock desaturated to a significant extent also in this test case. In CEA results as well as in these from the Couplex-Gaz the host rock desaturation was very weak. Indeed, due to very low permeability of the clay and its steep capillary pressure curve, the long distance and high amplitude desaturation is not expected to occur. This behaviour of the *MiGasTra* code may result from the numerical diffusion associated with upwinding strategy of the convection terms. In future work this point will be further investigated.

As a conclusion IRSN shall recall that the code they have tested on the calculations cases of PAMINA WP3.2 has proved to be efficient and stable, allowing obtaining numerical solutions up to an arbitrary time even with very strong parameter contrasts. The results that were obtained are similar to those of other groups. However some differences with the CEA and SCK·CEN simulations exist. In the Supercontainer case the gas overpressure was find similar as well the saturation evolution at short times. However the full resaturation state was not reached in the IRSN simulations up to 1’000’000 years (versus 320’000 years by CEA), which may be due to the planar geometry used by IRSN, versus axis-symmetrical one applied by CEA. SCK·CEN has conducted its simulations with a stronger gas production and with fully saturated initial conditions making any comparison quite problematical. However, the gas overpressure that they obtain is not very different and seems to be limited by the hydrogen dissolution in water. In the second test case (Couplex-Gaz), the simulations done by CEA diverged at 350 years, thus it was only possible to compare the evolution of the systems during this short period. A significant desaturation of the host rock was observed in this test case (IRSN results). This may indicate that the upwinding strategy IRSN use is inappropriate for this kind of system since it generates too much of numerical diffusion. Further investigations are needed to clarify this point.

Appendix D Summary of the contribution of NRI

During the work package 3.2 of RTDC-3 of the PAMINA integrated project, the following models were created:

- A simple model of gas diffusion transport through the bentonite (in *GoldSim*).
- A model of diffusional transport of hydrogen from steel canister walls for one borehole (in *GoldSim*).
- A simple model of two-phase flow from a wall of steel canister through the bentonite (in *TOUGH2*).
- A two phase flow hydrogen transport for one borehole with damaged container (in *TOUGH2*).

The models are based on a set of experiments for simulating of hydrogen generation and transport through the bentonite, which were performed in NRI laboratory. Data obtained in these experiments were described and analyzed for this work package. All models correspond to the Czech concept of deep geological repository.

The main modelling results are the following:

- Diffusion transport of hydrogen through bentonite is limited by bentonite-granite and bentonite-cement interfaces and gas generated by corrosion of canisters with assumed rate above 0.025 μm/a cannot be removed fully from the container walls by diffusion in water.
- Two-phase flow hydrogen transport is very slow, there is no sufficient amount of generated hydrogen for quick breakthrough as it is in laboratory experiments, so bentonite buffer should not be damaged.

Appendix E Summary of the contribution of SCK·CEN

In this study, several aspects in the assessment of the impact of gas generation were examined by means of a case study focussing on deep disposal of Supercontainers containing vitrified HLW in Boom clay. In general, anaerobic corrosion of steel EBS components is found to be the main source of gas generation (in this case hydrogen) in the near field of a radwaste repository.

The evolution of the EBS in terms of its water saturation, pressure and temperature is quite complex and it is of importance to know the prevailing conditions at the on-set of gas generation. As a first step, resaturation calculations were performed, to find out whether or not near field temperatures are still significantly increased at the start of anaerobic gas production. Note that full saturation is only roughly indicative for the transition of oxidising to reducing conditions, which could be considered as the start of the anaerobic corrosion reaction. Furthermore, since there is still substantial uncertainty on the hydraulic properties of the EBS materials and their initial saturation degree, these resaturation calculations considered a broad range of possibilities. In the most likely case, combining a hydraulic conductivity comparable to the one of Boom clay with a high initial saturation (80%), the whole gallery would be saturated with pore water within a couple of years. This means that temperatures are at their maximum when corrosion gas production starts.

The corrosion gas source term was implemented using different assumptions; namely two constant corrosion rates of 0.1 µm/year and 1 µm/year and a transient case where the influence of temperature on the corrosion process was assessed through application of the Arrhenius law. Next, it was assessed whether the generated hydrogen could be evacuated by diffusion as dissolved species, by comparison of cumulative gas production rates and the maximum rate at which dissolved hydrogen can diffuse away from the source. In these simplified transport simulations two values of diffusion coefficients were tested: a D_p of 5×10^{-10} $m^2 \cdot s^{-1}$ and a D_p of 5×10^{-11} $m^2 \cdot s^{-1}$. The results showed that for some calculation cases, diffusion alone is not enough to dissipate the gas produced within the EBS. However, there was no indication that a free gas phase could extend into the Boom Clay, i.e. free gas, if any, should only be found within the EBS.

A detailed multiphase flow analysis comprised the next step in this study. The aim of these fully coupled two-phase flow calculations was to assess the evolution of pressure, saturation and temperature in the repository and its environment. However, the emphasis was on gaining insight in the possible behaviour of the system, and in particular testing the robustness of the system by using a variety of source term formulations and bounding values of the buffer permeability. In addition, the impact of heat generation was examined. Results of these calculations show that the influence of temperature on the gas production process could be substantial (Arrhenius law) but the overall influence of temperature on the gas transport process is small. The implementation of a heat source results in a slightly increased total pressure, mainly due to thermal expansion of both water and gas phase. The degree of gas saturation is not significantly higher compared to the isothermal case. In case of a high-permeability buffer, thermal expansion of the pore water causes slightly higher water pressures, whereas the pressure increase was considerably higher in the low-permeability case. However, this could be a consequence of the sequential modelling of the resaturation process and the gas generation and transport in a heated saturated environment: in reality, with a low-permeability buffer, the resaturation process will take longer (estimated here at 20 to 80 years depending on initial saturation degree), and the temperatures will already be much lower. Besides, the behaviour of the solid phase (concrete, clay) in this model is greatly simplified through the use of a storage coefficient approach. In other words, only one-way fluid to solid coupling is considered, under an implicit constant total stress assumption.

In all considered cases, the presence of a gas phase remains very local, i.e. within the EBS, and the Boom clay is not subject to a pressure increase (which was already indicated by the simplified diffusive mass-balance calculations). In the most realistic case, the maximum gas pressure reaches 2.85 MPa in the concrete filler after 20 years of gas production. The corresponding gas saturation is 20%. The tensile strength of concrete of reasonable quality should be larger than the expected gas pressure.

Briefly summarised, the conclusions of this case study could be formulated as follows:

- Under the current assumptions, disposal of vitrified HLW in Boom Clay using a Supercontainer as waste package is not likely to pose a hydrogen gas problem due to anaerobic corrosion (which confirms the results obtained in the framework of EC project NF-PRO).
- A free gas phase may develop inside the concrete buffer, but the tensile strength of concrete should normally be larger that the expected gas pressure. Hence, gas-induced fracturing should be unlikely.
- The mechanical and hydraulic integrity of the Boom clay should thus not be threatened.

Moreover, some conservative assumptions to the conceptual model are worth mentioning:

- the corrosion rate was neither dependent on the degree of saturation nor on H_2 pressure
- consumption of H_2O by the anaerobic corrosion reaction was not taken into account, although this is not believed to have a large influence on the results.

It is to be noted, however, that other waste types, particularly intermediate-level wastes, might be more critical with respect to gas production and especially gas production rate than the vitrified high-level waste considered in these exploratory calculations.

These calculations have further shown that it is feasible to improve certain formulations in the constitutive laws of *TOUGH2*. An example was discussed in which results of a more accurate temperature dependency of the hydrogen solubility were compared to the standard simplified formulation. However, the nature of the curve is such that the influence on the final timing and amplitude of pressure build up is negligible.

Finally, two numerical tools, *TOUGH2* and *Code Bright*, are mutually verified through three benchmark cases based on the considered case study: 1) HG coupled model for a 1D problem; 2) HG coupled model for a 2D axi-symmetrical problem; 3) THG coupled model for a 2D axi-symmetrical problem. Comparisons between numerical results demonstrate that these two numerical tools produce similar results in all three benchmarks. The minor differences between results obtained from the two numerical tools are in part due to the different discretizing method and numerical techniques, and in part due to several different constitutive laws. *Code Bright* seems to be quite sensitive to convergence parameters. During the calculation, convergence problems have been encountered occasionally. The results reflect sharp oscillations at some critical points, while results from *TOUGH2* seem to be more stable. However, the advantage of *Code Bright* is that it has provisions for solving mechanically coupled problems, and is easier to be implemented with self-defined constitutive laws.

As an overall conclusion, the achievements within this work package have shown that the tools applied are adequate (selected processes of concern in gas generation and dissipation – dissolution, diffusion and two-phase flow, if necessary coupled to heat transport – can be implemented), accurate (numerical results of both codes in good agreement) and versatile. However, the challenging task of proving that the conceptual model is comprehensive still remains. Substantial efforts are still necessary in the domains of model qualification and, if possible, validation. In this respect, much is expected from the recently started EU-FP7 FORGE project ("Fate of Repository Gases"), in which the various models for the gas generation and migration will be benchmarked to experiments and in which process level knowledge will be further developed.

References

[1] Huertas, F., M.V. Villar, J.L.Garcia-Siñeriz, P. Sellin, D. Stührenberg, and H.-J. Alheid, 2008. Final Synthesis Report RTD Component 3: Thermo-hydro-mechanical (geochemical) processes in the engineered barrier system; NF-Pro Deliverable report D3.6.2

[2] Alonso, J., P. de Preter, A. Hooper, H. Umeki, A. Van Luik, P. Zuidema, S. Voinis, C. Pescatore, T. Sumerling, and P. Smith, 2004: Post-Closure Safety Case For Geological Repositories, Nature And Purpose, NEA report 3679, ISBN 92-64-02075-6

[3] Horseman, S.T., J.J.W. Higgo, J. Alexander, and J.F. Harrington, 1996: Water, gas and solute movement through argillaceous media, OECD/NEA Report CC-96/1, Paris,

[4] Harrington, J.F., and S.T. Horseman, 2003: Gas Migration in KBS-3 Buffer Bentonite, SKB Technical Report TR-03-02, Stockholm, Sweden

[5] NEA, 2001: Radioactive Waste Management. Gas Generation and Migration in Radioactive Waste Disposal. Safety-relevant Issues. Workshop Proceedings, Reims, France, 26-28 June 2000. OECD publishing, ISBN 9789264193086

[6] Rodwell, W., S. Norris, W. Cool, M. Cuñado, L. Johnson, M. Mäntynen, W. Müller, P. Sellin, M. Snellman, J. Talandier, T. Vieno, and S. Vines, 2003: A thematic network on gas issues in safety assessment of deep repositories for radioactive waste (GASNET). Final Report, European Commission, EUR 20620EN, 45 p.

[7] Manai, T., 1995: EVEGAS (European Validation Exercise of GAS migration model through porous media) CEC contract FI2W-CT93-0125

[8] Ortiz, L., G. Volckaert, P. De Cannière, M. Put, M.A. Sen, S.T. Horseman, J.F. Harrington, M. Impey, and S. Einchcomb, 1997: MEGAS: modelling and experiments on gas migration in repository host rocks, EUR 17453

[9] Haijtink, B. and W.R. Rodwell, 1996: Projects on the effects of gas in underground storage facilities for radioactive waste (Pegasus project) EUR 16746

[10] Haijtink, B. and W.R. Rodwell, 1998: Projects on the effects of gas in underground storage facilities for radioactive waste (Pegasus project) EUR 18167

[11] Nordbotten J.M., I. Aavastsmark, and G.T. Eigestad, 2007: Monotonicity of control volume methods. Numerische Mathematik, 106, p. 255-288

[12] National Cooperative for the Disposal of Radioactive Waste (NAGRA), 2002: Project Opalinus Clay: Safety report. Demonstration of disposal feasibility for spent fuel, vitrified high-level waste and long-lived intermediate-level waste (Entsorgungsnachweis). Nagra Technical Report NTB 02-05, Wettingen, 2002.

[13] FORGE project website (2009). http://www.bgs.ac.uk/forge/

[14] Norris, S., 2008: Uncertainties Associated with Modelling the Consequences of Gas PAMINA Deliverable report D2.2.B.2

[15] Van Genuchten, M. 1980: A Closed-Form Equation for Predicting the Hydraulic Conductivity of Unsaturated Soils, Soil Sci. Soc., 44, p. 892-898

[16] Corey, A. 1954: The Interrelation Between Gas and Oil Relative Permeabilities, Producers Monthly, November, p. 38-41

[17] Navarro, M., 2009: Simulating the migration of repository gases through argillaceous rock by implementing the mechanism of pathway dilation into the code *TOUGH2* (*TOUGH2-PD*). PAMINA Milestone report M 3.2.14

[18] Swift, B.T., A.R. Hoch, and W.R. Rodwell, 2001: Modelling gas migration in compacted bentonite: GAMBIT Club Phase 2 Final Report, Posiva Oy, Posiva 2001-02, 151 p.

[19] Hoch, A.R., K.A. Cliffe, B.T. Swift, and W.R. Rodwell, 2004: Modeling Gas Migration in Compacted Bentonite: GAMBIT Club Phase 3 Final Report, Posiva Oy, Posiva 2004-02

[20] Marschall, P., S.T. Horseman, and T. Gimmi, 2005: Characterisation of Gas Transport Properties of the Opalinus Clay, a Potential Host Rock Formation for Radioactive Waste Disposal, Oil and Gas Science and Technology - Rev. IFP, Vol. 60, No. 1, p. 121-139

[21] Mazurek, M., F.J. Pearson, G. Vockaert, and H. Bock, 2003: Features, Events and Processes Evaluation Catalogue for Argillaceous Media, OECD/NEA, 376 p.

[22] Weetjens, E., J. Perko, and X. Sillen, 2006: Project internal report on "gas production and transport" interim results. PAMINA Milestone report M 3.2.7

[23] Perko, J. and E. Weetjens, 2008: Notes on the effect of temperature dependent hydrogen solubility in modelling gas dissipation. PAMINA Milestone report M 3.2.15

[24] Weetjens, E., J. Perko, and L. Yu, 2009: Final report on gas production and transport. PAMINA Milestone report M 3.2.16

[25] Commissariat à l’Energie Atomique (CEA), 2008: First results of calculations on gas production and transport. PAMINA Milestone report M 3.2.3

[26] Institut de Radioprotection et de Sûreté Nucléaire (IRSN), 2009: Internal report on "gas production and transport”. PAMINA Milestone report M 3.2.9

[27] Commissariat à l’Energie Atomique (CEA), 2009: Internal report on "gas production and transport". PAMINA Milestone report M 3.2.10

[28] Smaï, F. 2009: A model of multiphase flow and transport in porous media applied to gas migration in underground nuclear waste repository. *C.R. Acad. Sci. Paris, Ser. I,* 347 (9-10), p. 527-532

[29] Navarro, M., 2008: Implementing the process of pressure-induced dilation of gas pathways into the code *TOUGH2*. Internal report on model implementation and initial code testing. PAMINA Milestone report M 3.2.13

[30] Lukin, D. and A. Vokál, 2008: Conceptual model and prelimary results for gas generation and transport in SNF - carbon steel canister - bentonite buffer and backfill - granite host rock concept. PAMINA Milestone report M 3.2.6

[31] Lukin, D., 2009. The quantification of gas generation and migration in SNF - carbon steel canister - bentonite - granite concept - final results and report. PAMINA Milestone report M 3.2.8

[32] Wickham, S.M., M.B. Crawford, and D.G. Bennett, 2005: Belgian Supercontainer Design for HLW and Spent Fuel Disposal. Evaluation of the Reference Design. Galson Sciences LTD, Oakham

[33] Wickham, S.M., 2005: The ONDRAF/NIRAS Supercontainer Concept. Galson Sciences LTD, Oakham

[34] Runchal, A.K., 1997: *PORFLOW*, a Software Tool for Multiphase Fluid Flow, Heat and Mass Transport in Fractured Porous Media. User's manual, Version 3.07. ACRi, Bel Air

[35] COMSOL, 2005: *COMSOL* Multiphysics 3.2, Earth Science Module User's Guide, COMSOL AB, Stockholm, Sweden

[36] Volckaert, G. and D. Mallants, 1999: De gasproblematiek bij het bergen van radioactief afval in een diepe berging in de Klei van Boom. SCK•CEN report R-3287, Mol

[37] Pruess, K., C. Oldenburg, and G. Moridis, 1999: *TOUGH2* User's Guide, version 2.0. Lawrence Berkeley National Laboratory, Berkeley

[38] Pruess, K., 2004: The *TOUGH* codes - a family of simulation tools for multiphase flow and transport processes in permeable media. Vadoze Zone Journal 3, p. 738-746

[39] http://www-cast3m.cea.fr/

[40] Amaziane, B., M. Dymitrowska, M. El Ossmani, and C. Serres, 2007 : Un schema Volume Finis Pour le Benchmark Couplex-Gaz. Workshop Couplex-Gaz, Orly, 4th and 5th of April 2007

[41] Talandier, J., 2005: Présentation d'un benchmark sur la simulation des écoulements biphasiques en milieu poreux: application au transfert des gaz autour du stockage de déchets radioactifs. Andra presentation, http://www.gdrmomas.org/Activites/2005/cirm05/exposes/expo-talandier.pdf

[42] ANDRA, 2005: Dossier 2005 Argile, ISBN 2-951 0198-8-5, 240 p.

[43] Golder Associates, 2007: GoldSim Contaminant Transport Module. User manual version 4.20

[44] Hoch A.R., Cliffe K.A., Swift B.T., Rodwell W.R., 2004: Modeling Gas Migration in Compacted Bentonite: Gambit Club Phase 3 Final Report, Posiva Oy, Posiva 2004-02

[45] Lukin, D. and A. Vokál, 2007: Preliminary compilation of relevant FEPs and data for gas generation and transport. PAMINA Milestone report M 3.2.5

[46] Blümling, P., F. Bernier, P. Lebon, and C.D. Martin, 2007: The excavation damaged zone in clay formations time-dependent behaviour and influence on performance assessment. Physics and Chemistry of the Earth, 32, p. 588 -599

[47] Navarro, M., E. Weetjens, A. Vokál and M. Dymitrowska, 2007: Calculation cases collection. PAMINA Milestone report M 3.2.1